GEM TN-93-445

GEM Magnetic Field (Reference for the Muon System)

S. Timofeev
SSC Laboratory

August 2, 1993

Abstract;

Overall map of the GEM magnetic field, radial distribution of the GEM magnetic field at Z positions correspond to the muon chamber superlayers positions, detailed distribution of the magnetic field in the barrel and endcap muon chambers, distribution and integral Bzdl of the magnetic field along the muon tracks at the different θ angles and axial nonsymmetry of the magnetic field are presented.

The 3-dimensional magnetic analysis of the GEM detector was carried out using the OPERA-3d prepocessor program, TOSCA analysis program and OPERA-3d postprocessor program on UNIX workstation.

Bz and Br components of the magnetic field have been calculated for the muon chambers placement regions.

GEM MAGNET SYSTEM.

GEM magnet system is a large superconducting solenoid assembly with field shaping in the forward region. The solenoid assembly is physically 31 m long with 18 m diameter inner bore and produces a central field of 0.8 Tesla. It consists of two half-length coil assemblies, each 14234 mm long, separated by a distance of 1532 mm at the midplane. In the forward direction the magnetic field is shaped to improve the muon resolution. This shaping is accomplished by large ferromagnetic structures, called Forward Field Shapers (FFS), which are roughly projective to the IP, coaxial with the beam axis, and occupy the volume from 10-18 m from the IP in both directions. The elevation view of the GEM magnet system is presented in Fig 1.

GEM MUON SYSTEM.

GEM muon system is a system of three superlayers, each containing multiple layers of detectors placed between the calorimeter and the solenoidal magnet coils. The positions of the muon chambers are indicated in Fig.2.

FEM MODEL

The procedure of the creating of the FEM model is described in (1). The final FEM-model that has been used for the analysis is presented in Fig.3. It consist from the 115710 elements (120120 nodes).

RESULTS.

The overall map of the GEM magnetic field is presented in Figs.4 Fig.4.1 represent the Bz component distribution, Fig.4.2 represent Br component distribution at the RZ plane of the half of the GEM sensitive volume (R=0-9000 mm; Z=0-17000 mm).The Forward Field Shapers (FFS) introduce a significant radial field component, the gap between the halfs of the coils lead to the decreasing of the field in this region, in the region of the last endcap muon chambers the radial component of the field change the sign that lead to the decreasing of the muon momentum resolution.

Figs.5 represent the radial distribution of the GEM magnetic field at Z positions correspond to the muon chamber superlayers positions (Z=0, -5760, -9950, -11250, -14750 and -16250 mm).

Figs.6 represent detailed distribution of the magnetic field in the barrel muon chambers and Figs.7 - in the endcap muon chambers.

The FFS support structure made from regular steel lead to the axial nonuniformity of the magnetic field in the endcap region. Figs.8 represent the worse case of the axial nonsymmetry of the magnetic field in the endcap region.

Distribution of the magnetic field along the muon tracks at the different θ angles (θ= 90; 29.60; 17.01; 9.75 and 9.45 grad) are presented in Figs.9.

Integrals Bzdl of the magnetic field along the muon tracks at the different θ angles (θ= 9.75; 30; 60; 90 grad) are presented in Fig.10.

REFERENCES:

1. S.Timofeev "Axial Symmetry of the GEM Magnetic Field" GEM TN-93-384.

LIST OF FIGURES:

Fig.1 The elevation view of the GEM magnet system .

Fig.2 The positions of the muon chambers.

Fig.3 FEM model.

Fig.4 Overall map of the GEM magnetic field.
- Fig.4.1 Bz component distribution.
- Fig.4.2 Br component distribution.

Fig.5 Radial distribution of the GEM magnetic field (Z positions correspond to the muon chamber superlayers positions).
- Fig.5.1 Z=0 ; R=0-9000 mm.
- Fig.5.2 Z=-5760 mm ; R=0-9000 mm.
- Fig.5.3 Z=-9950 mm ; R=1450-9000 mm.
- Fig.5.4 Z=-11250 mm ; R=1650-9000 mm.
- Fig.5.5 Z=-14750 mm ; R=2250-9000 mm.
- Fig.5.6 Z=-16250 mm ; R=2500-9000 mm.

Fig.6 Detailed distribution of the magnetic field in the barrel muon chambers.
- Fig.6.1 Internal layer: R=3854 mm.
- Fig.6.2 Middle layer: R=6282 mm.
- Fig.6.3 Outer layer: R=8588 mm.

Fig.7 Detailed distribution of the magnetic field in the endcap muon chambers.
- Fig.7.1 Z=-5760 mm.
- Fig.7.2 Z=-6600 mm.
- Fig.7.3 Z=-9950 mm.
- Fig.7.4 Z=-11250 mm.
- Fig.7.5 Z=-14750 mm.
- Fig.7.6 Z=-16250 mm.

Fig.8 Axial nonsymmetry of the magnetic field in the endcap region.
- Fig.8.1 overall picture of the local axial nonuniformity.
- Fig.8.1 axial nonuniformity for the last muon chamber superlayer.

Fig.9 Distribution of the magnetic field along the muon tracks at the different θ angles.
- Fig.9.1 θ= 90 grad.
- Fig.9.2 θ= 29.60 grad
- Fig.9.3 θ= 17.01 grad
- Fig.9.4 θ= 9.75 grad
- Fig.9.5 θ= 9.45 grad

Fig.10 Distribution and integral Bzdl of the magnetic field along the muon tracks at the different θ angles.

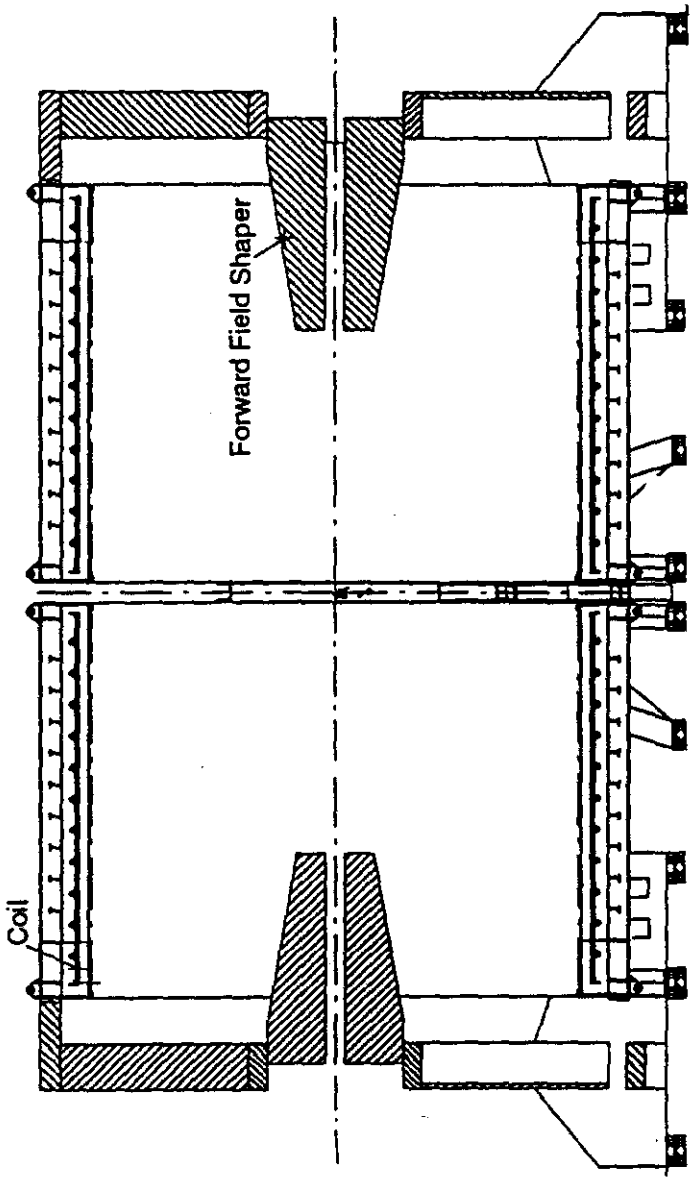

Fig.1

GEM DETECTOR PARAMETERS
BASELINE 2

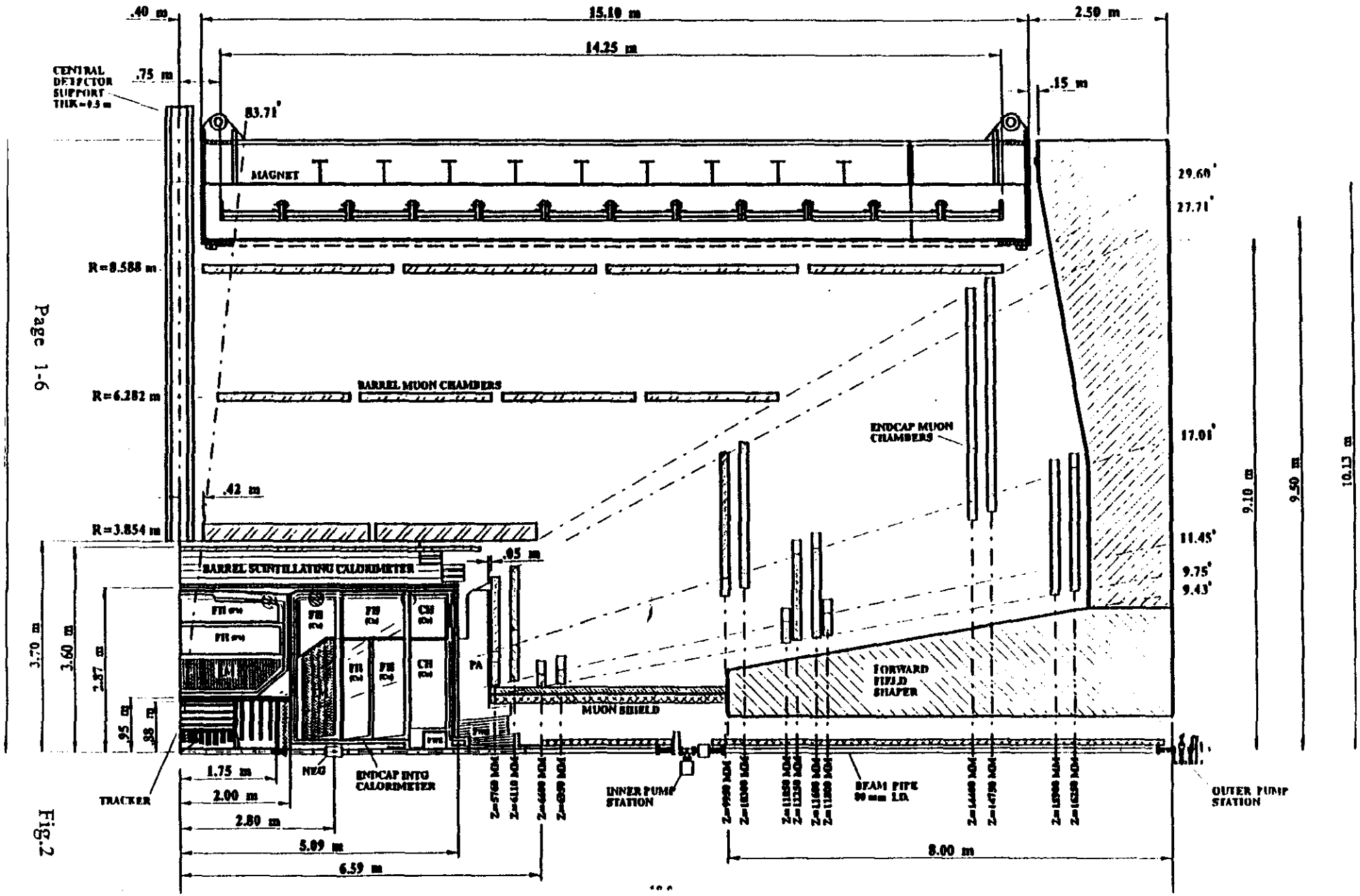

Fig.2

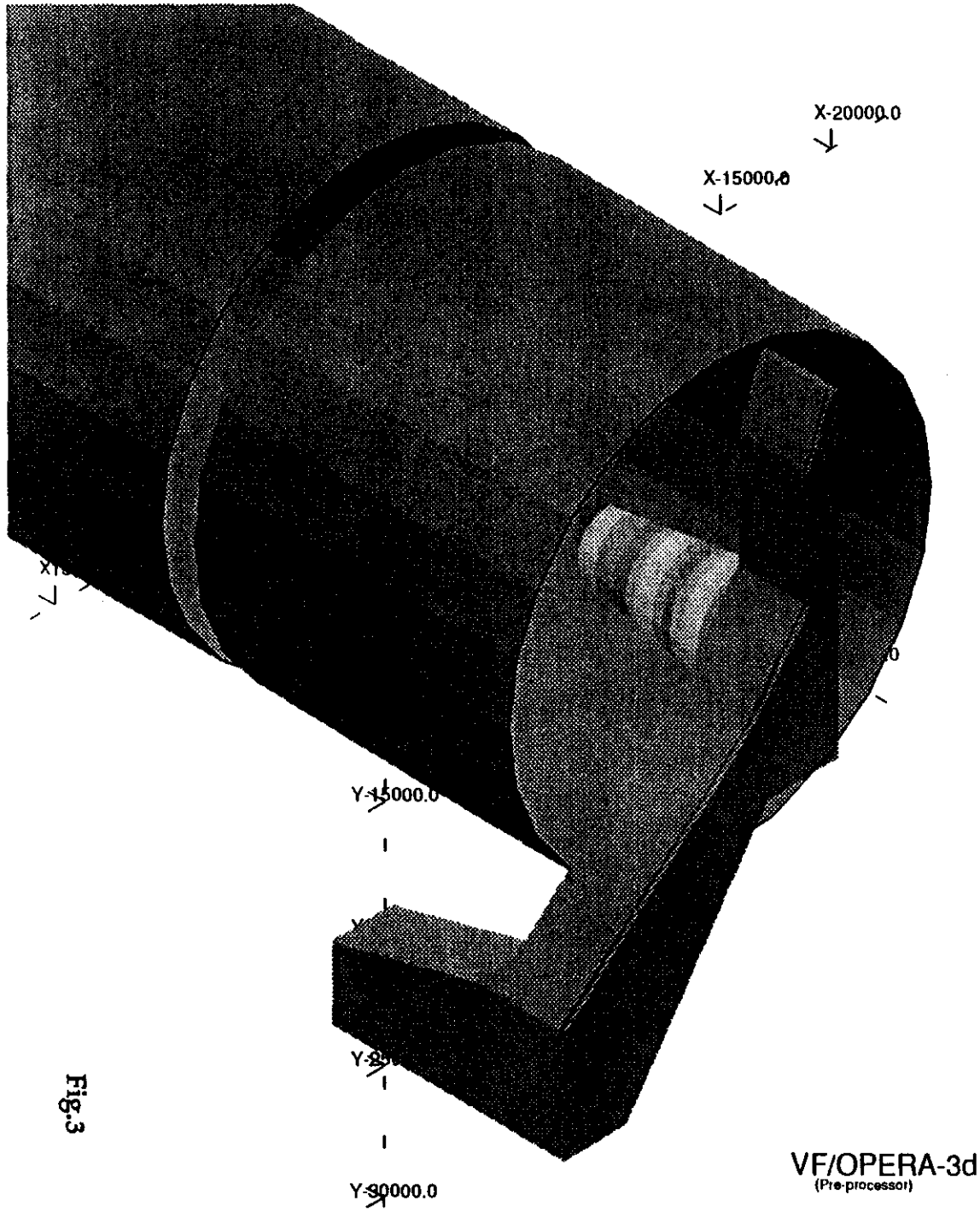

Fig.3

a.pic
27/Jul/93 15:51:21 Page 92 : hist comp=bz

Timofeev S.

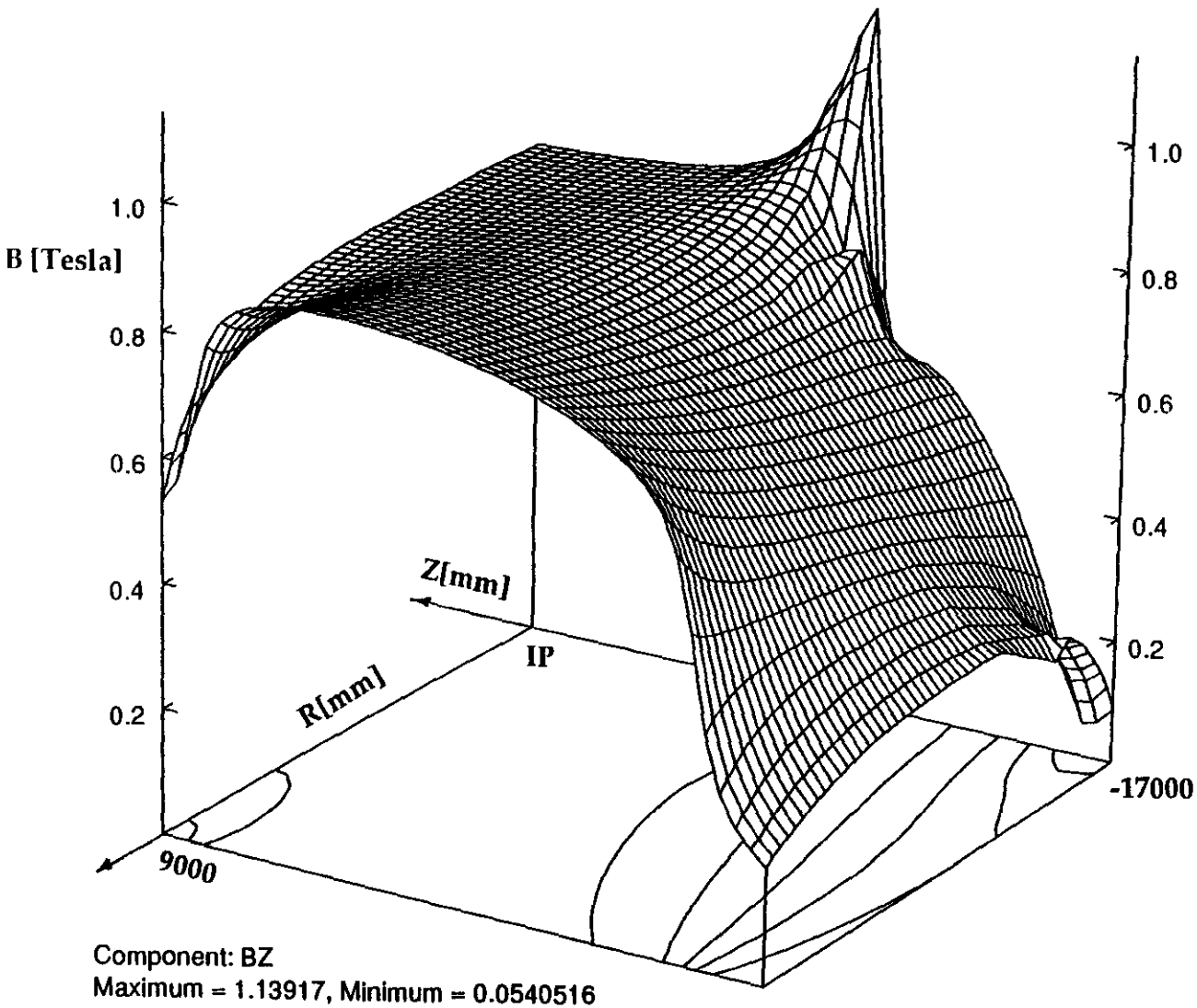

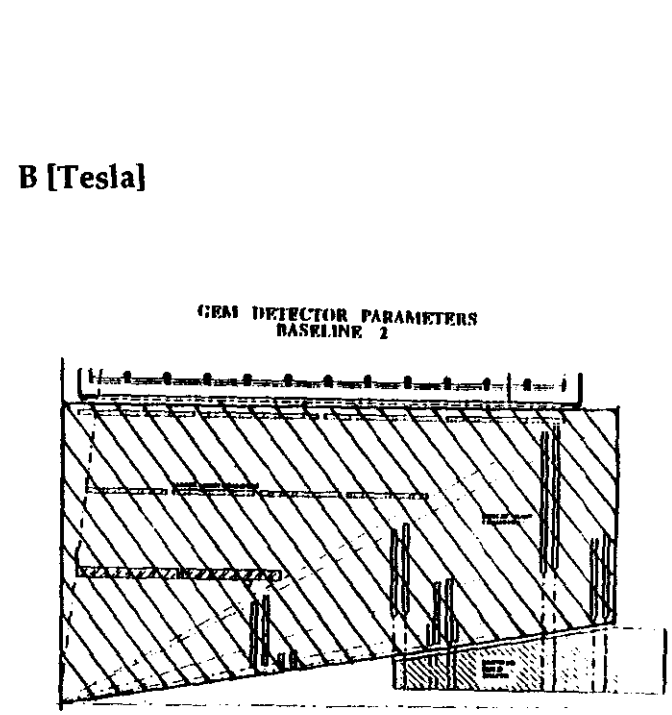

VF/OPERA-3d
(Post-processor)

Fig.4.1

a.pic
27/Jul/93 15:51:08 Page 91 : hist

Timofeev S.

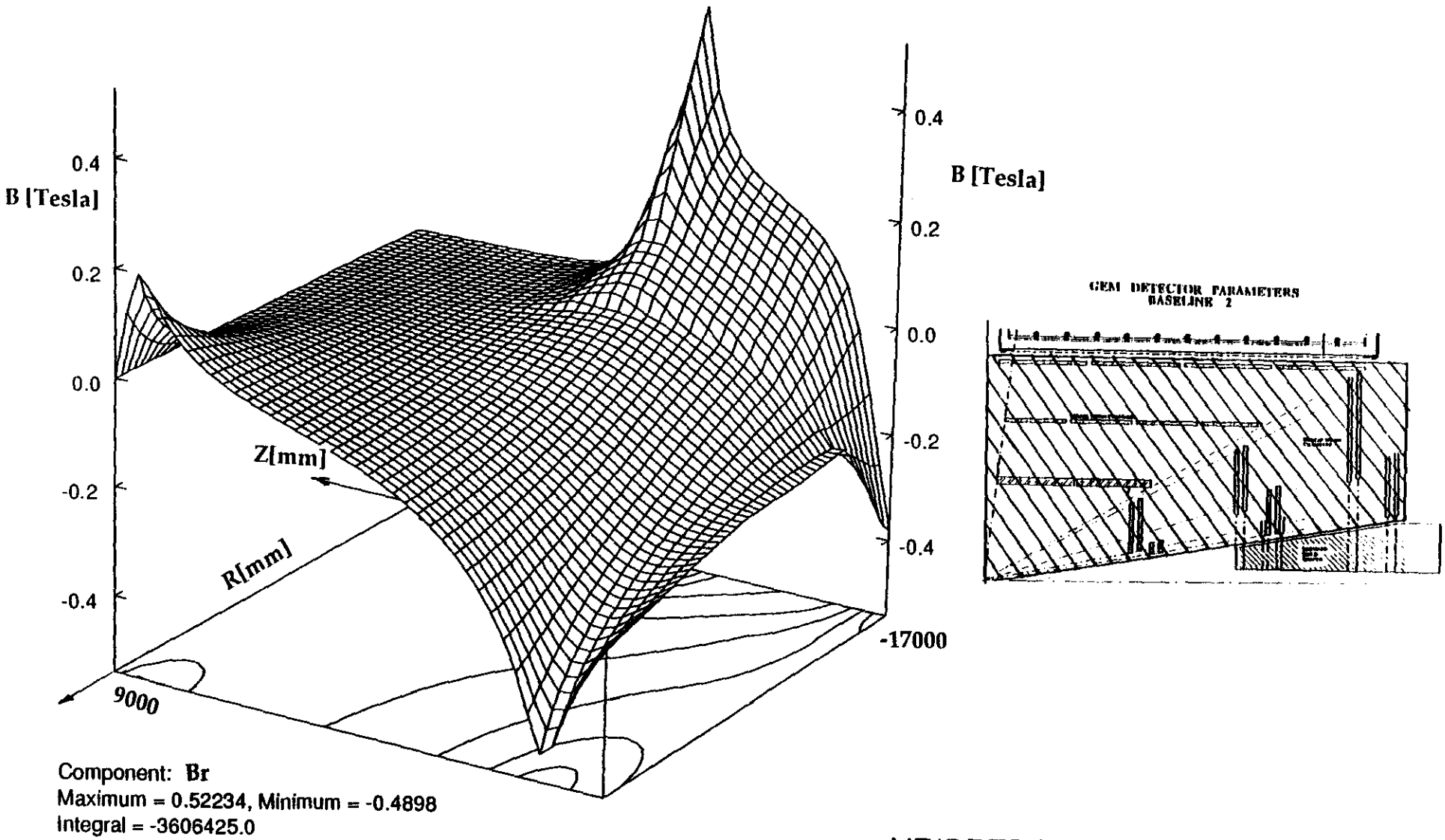

Component: Br
Maximum = 0.52234, Minimum = -0.4898
Integral = -3606425.0

VF/OPERA-3d
(Post-processor)

Fig.4.2

z0.pic
27/Jul/93 15:05:12 Page 41 : plot comp=bz

Timofeev S.

Z=0 mm

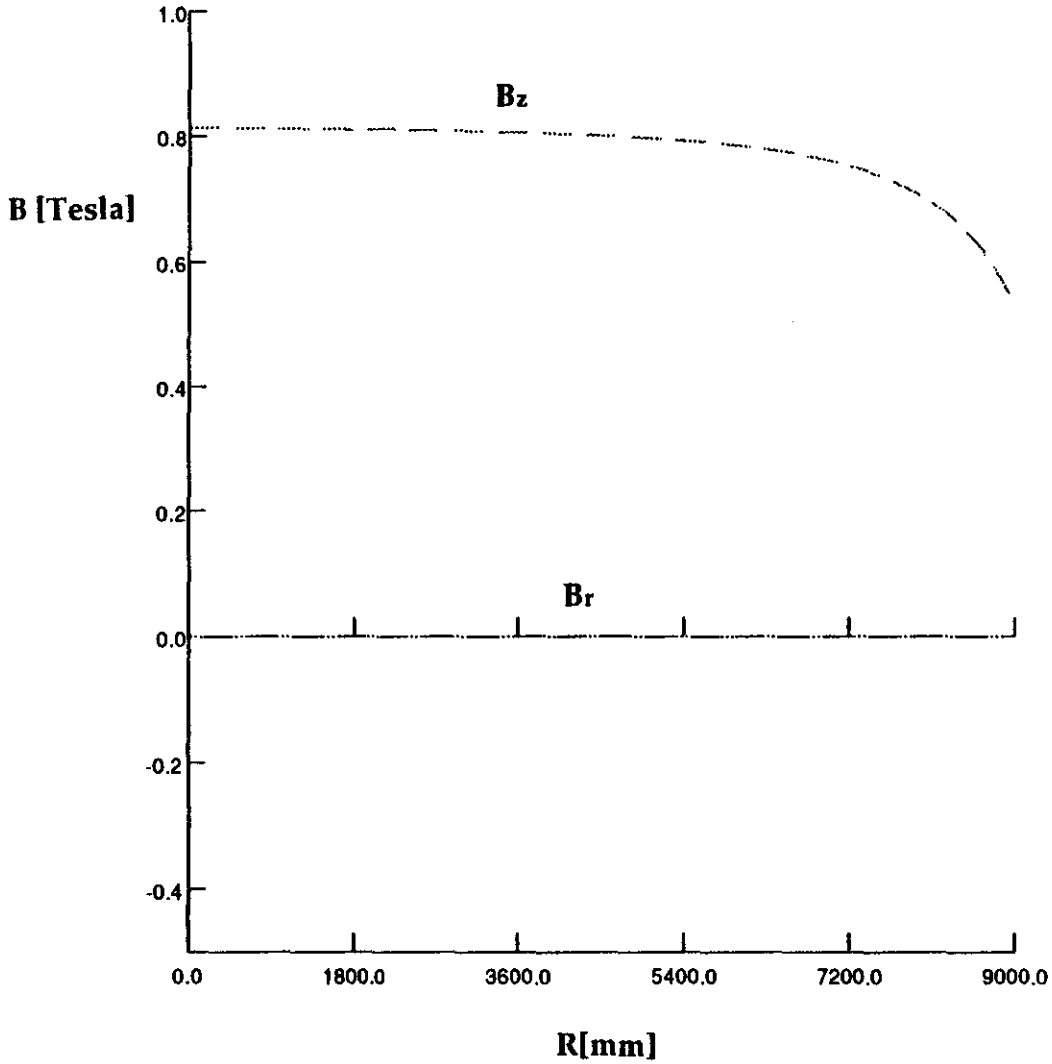

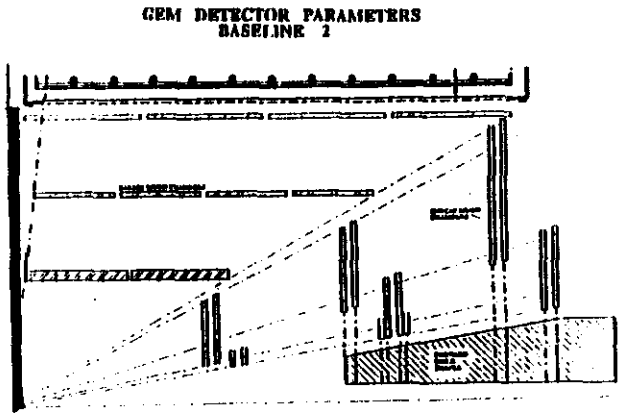

VF/OPERA-3d
(Post-processor)

Fig.5.1

z5760.pic
27/Jul/93 15:07:08 Page 44 : plot comp=bz

Timofeev S.

Z=-5760 mm

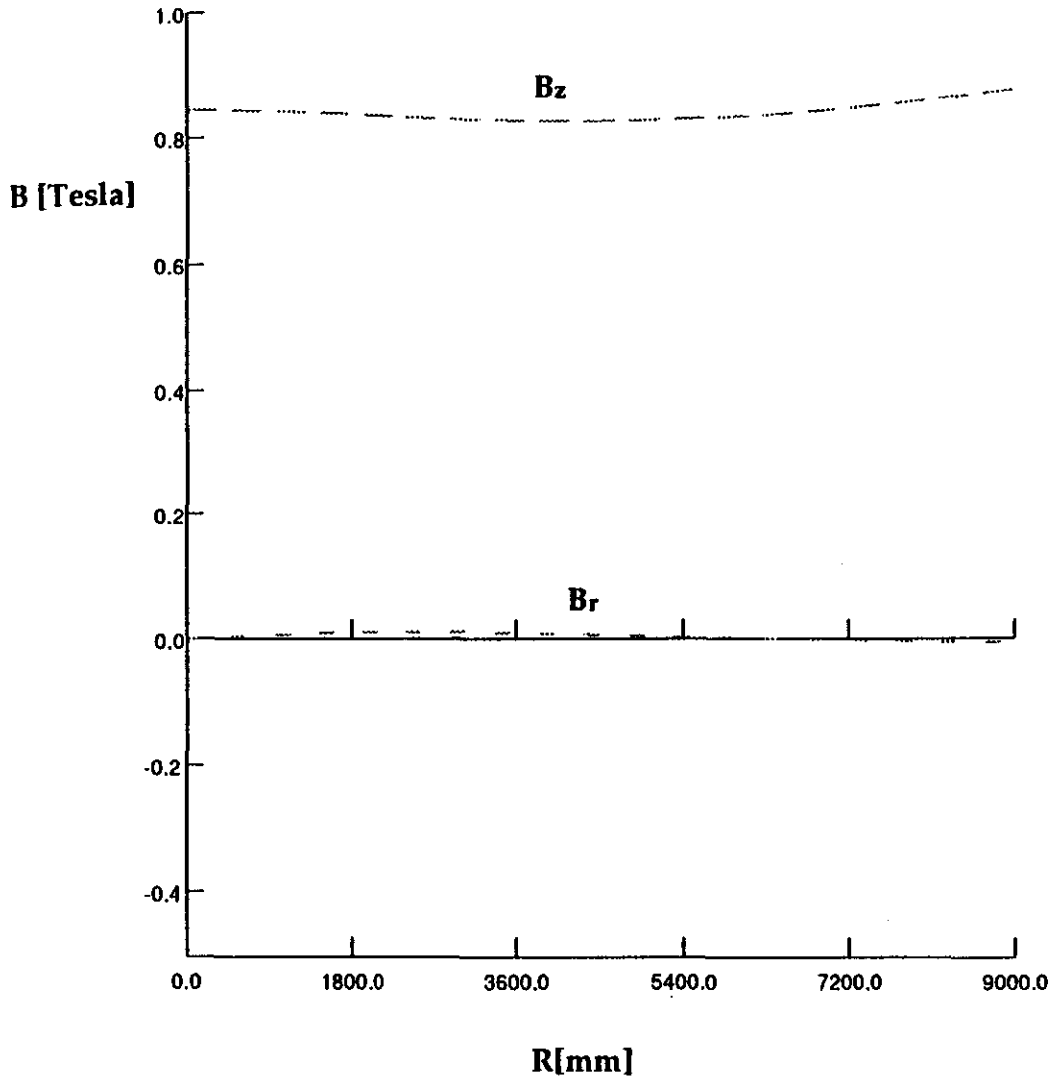

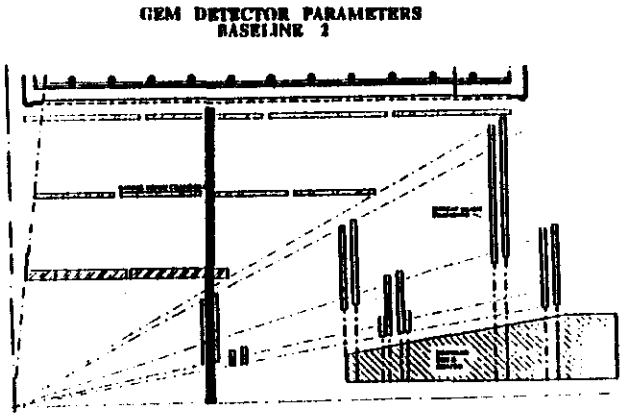

VF/OPERA-3d
(Post-processor)

Fig.5.2

z9950.pic
27/Jul/93 15:14:58 Page 53 : plot comp=bz

Timofeev S.

Z=-9950 mm

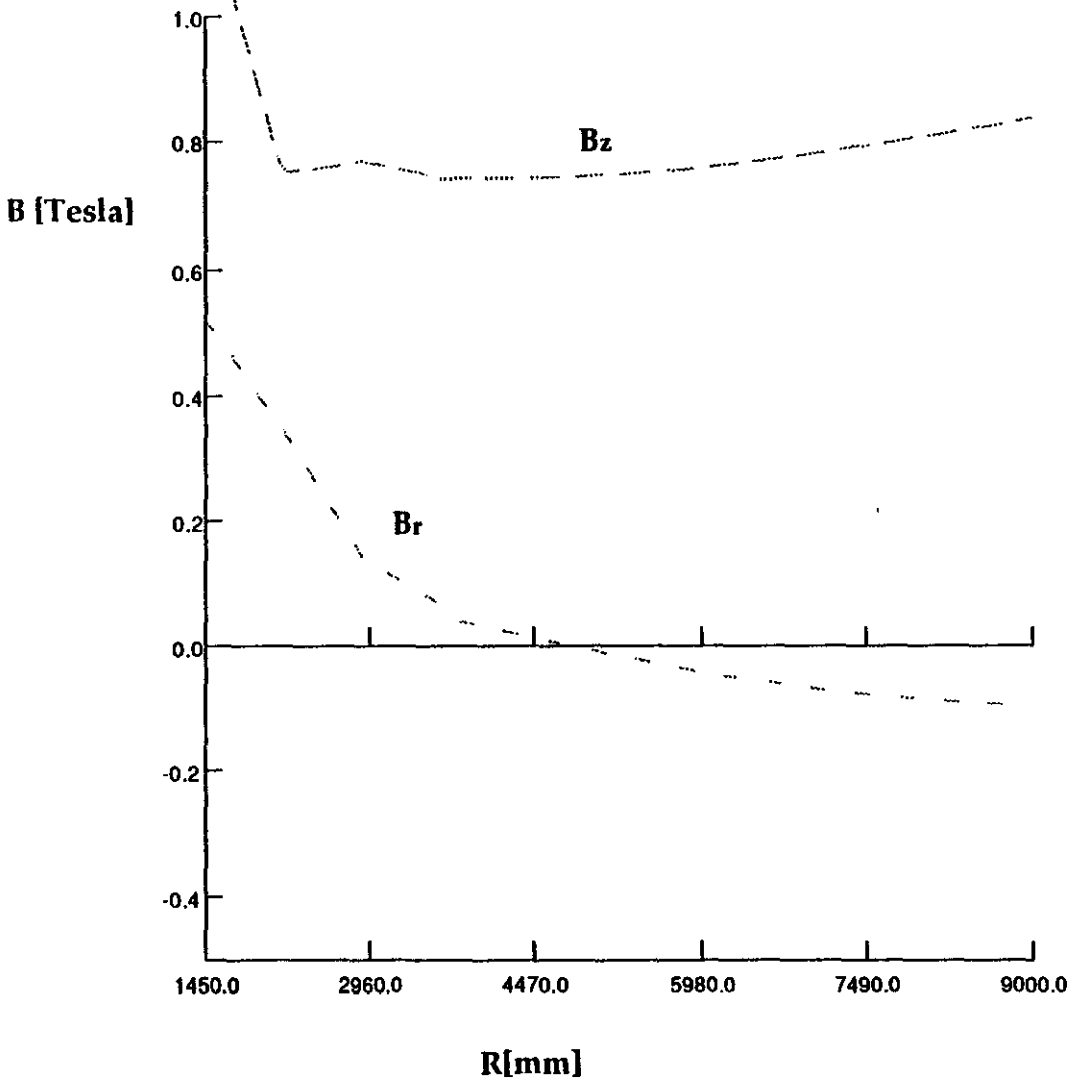

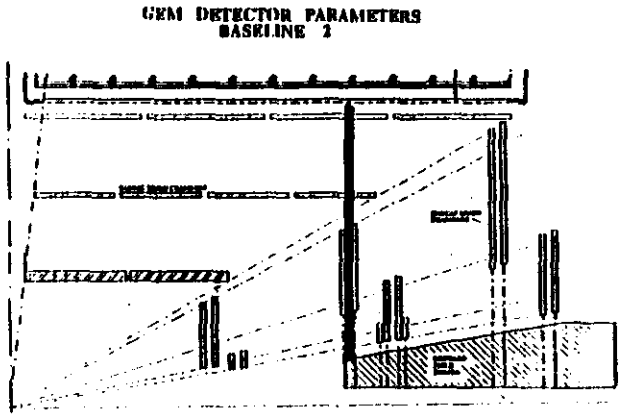

VF/OPERA-3d
(Post-processor)

Fig.5.3

z11250.plc
27/Jul/93 15:18:30 Page 62 : plot

Z=-11250 mm

Timofeev S.

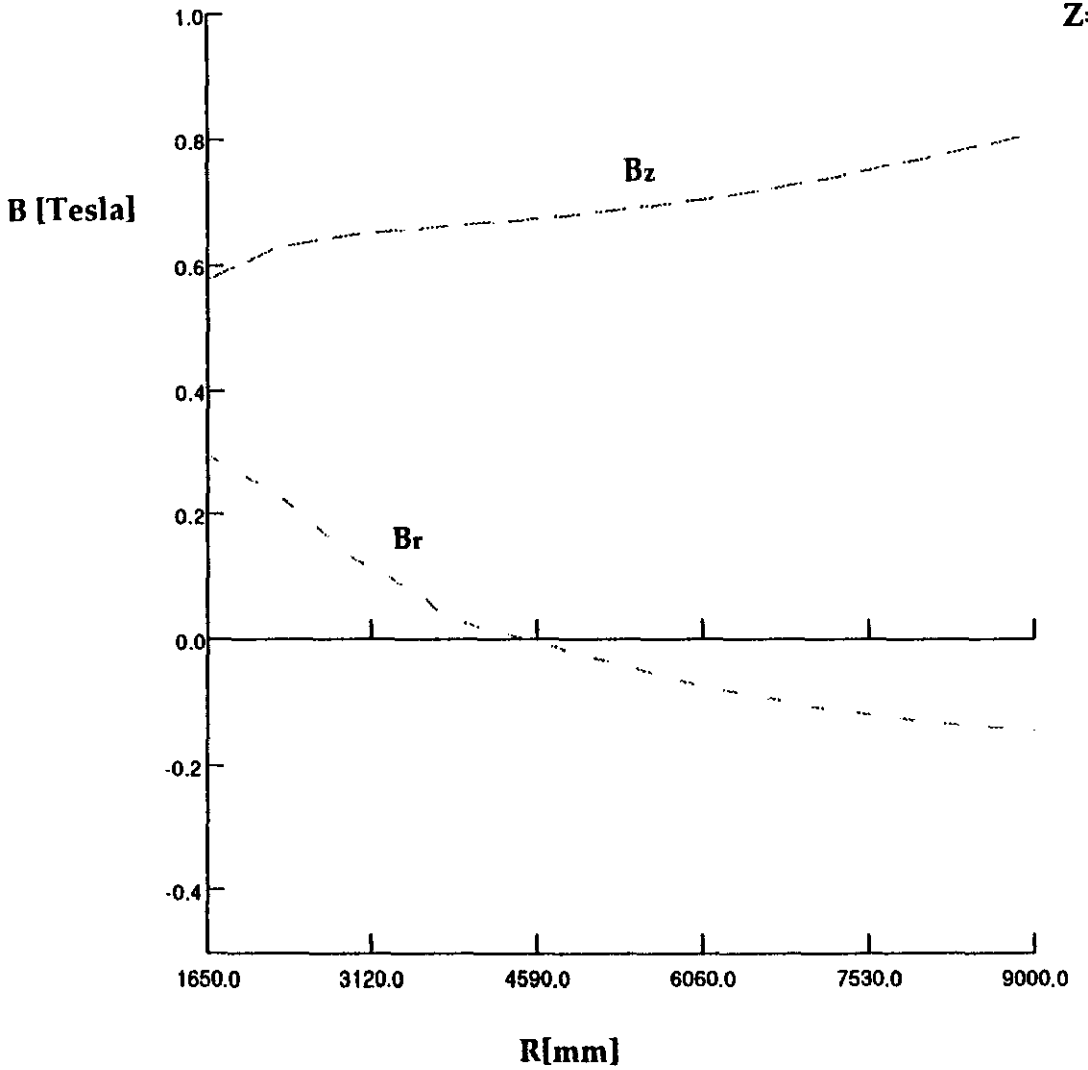

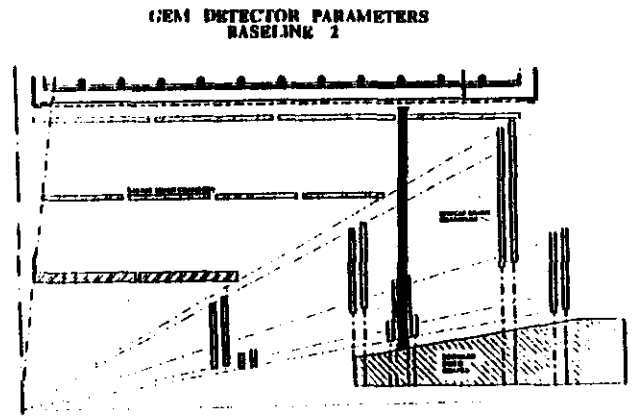

VF/OPERA-3d
(Post-processor)

Fig.5.4

z14750.plc
27/Jul/93 15:29:35 Page 71 : plot

Z=-14750 mm

Timofeev S.

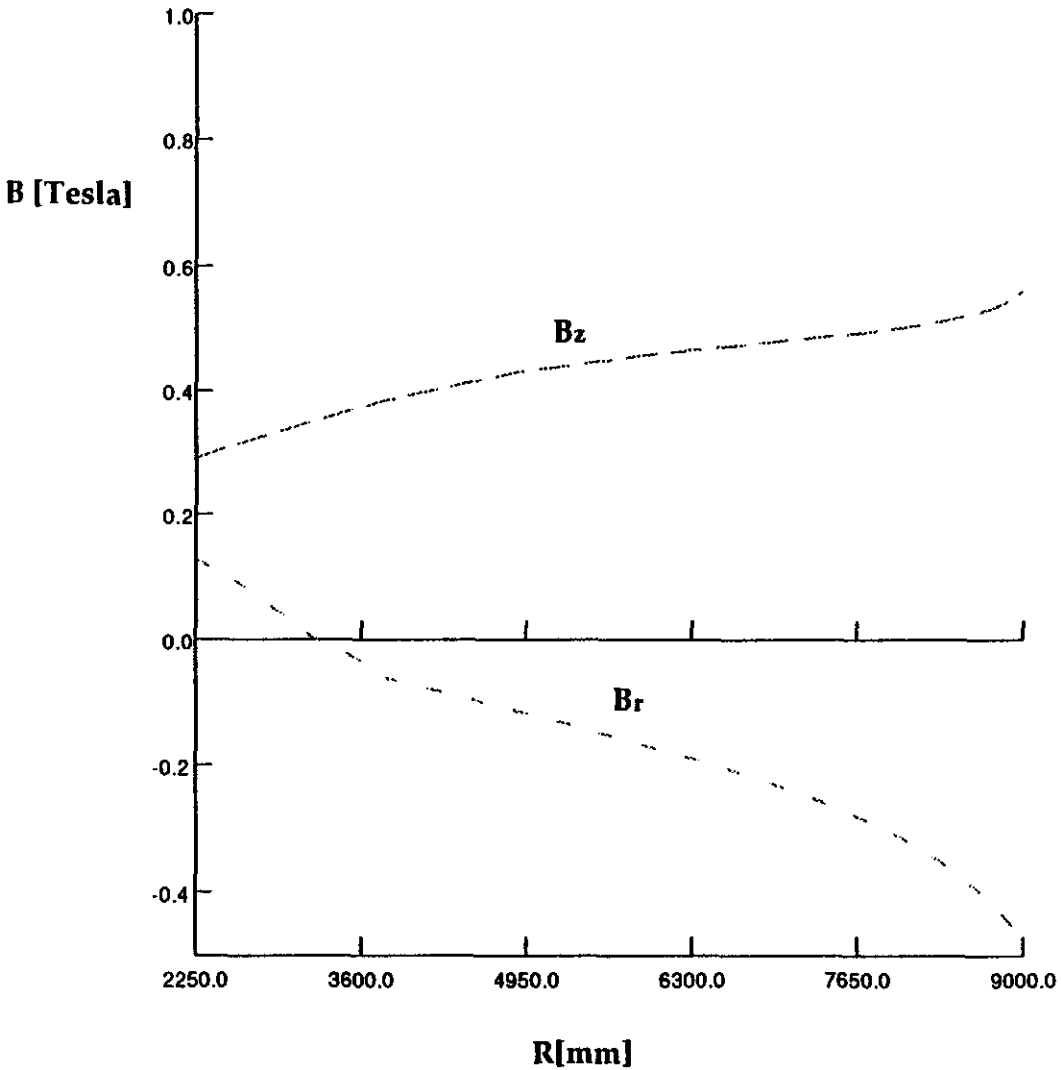

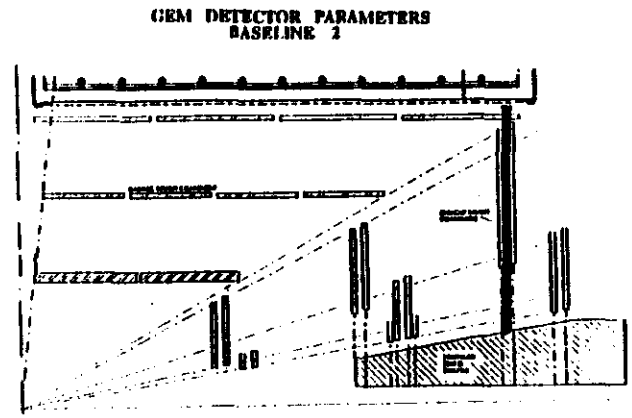

VF/OPERA-3d
(Post-processor)

Fig.5.5

z16250.pic
27/Jul/93 15:32:30 Page 79 : plot comp=bz

Timofeev S.

Z=-16250 mm

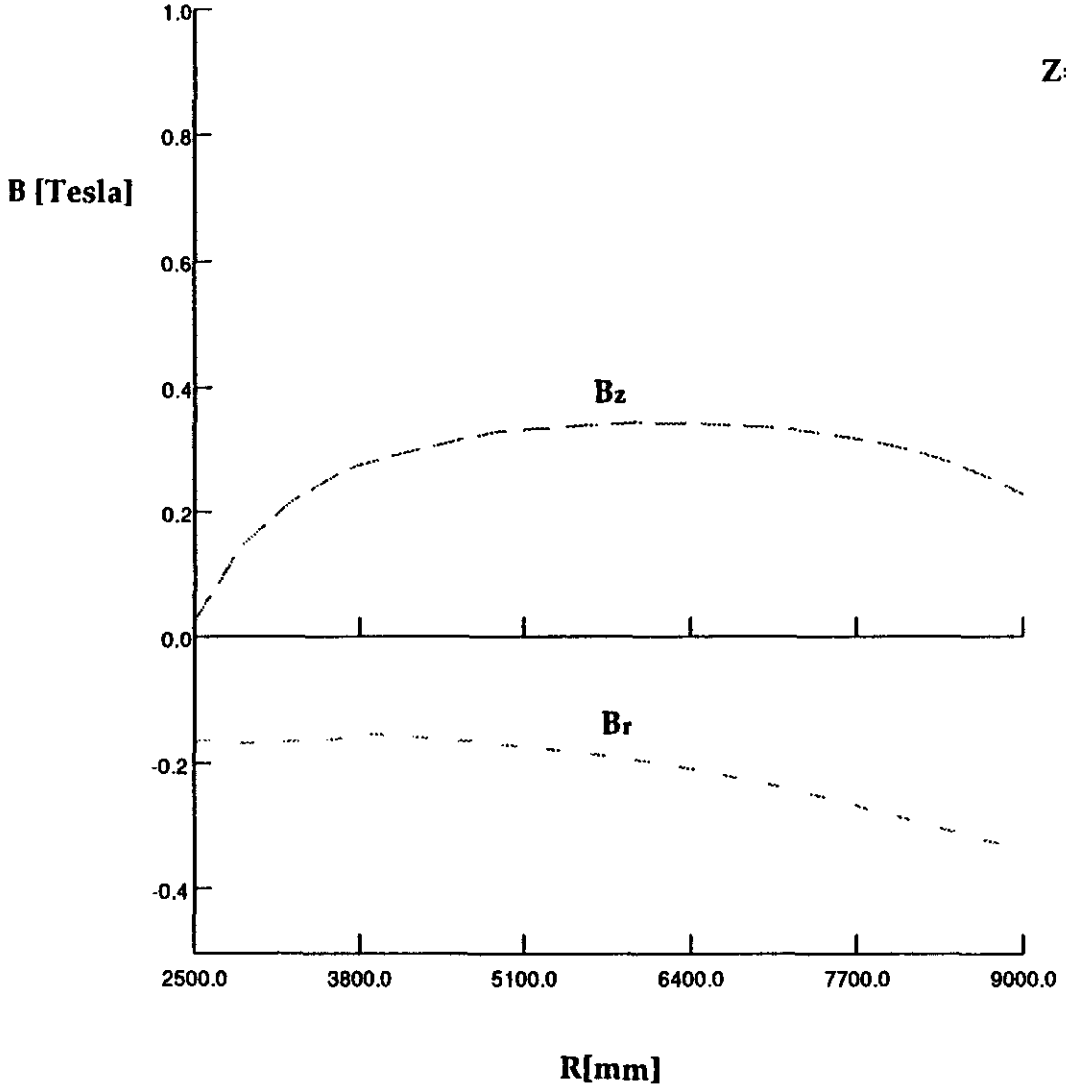

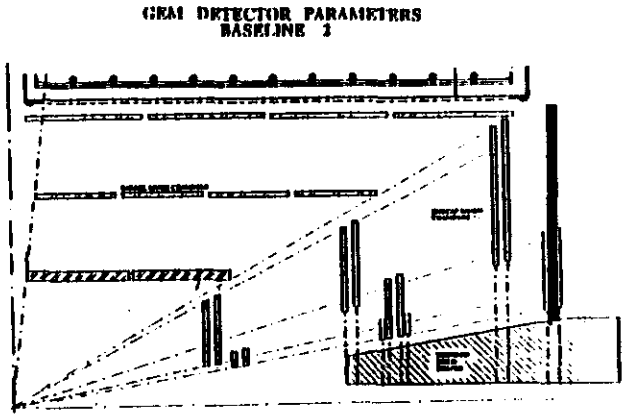

VF/OPERA-3d
(Post-processor)

Fig.5.6

r3854.plc
27/Jul/93 11:54:01 Page 35 : plot comp=bz

Timofeev S.

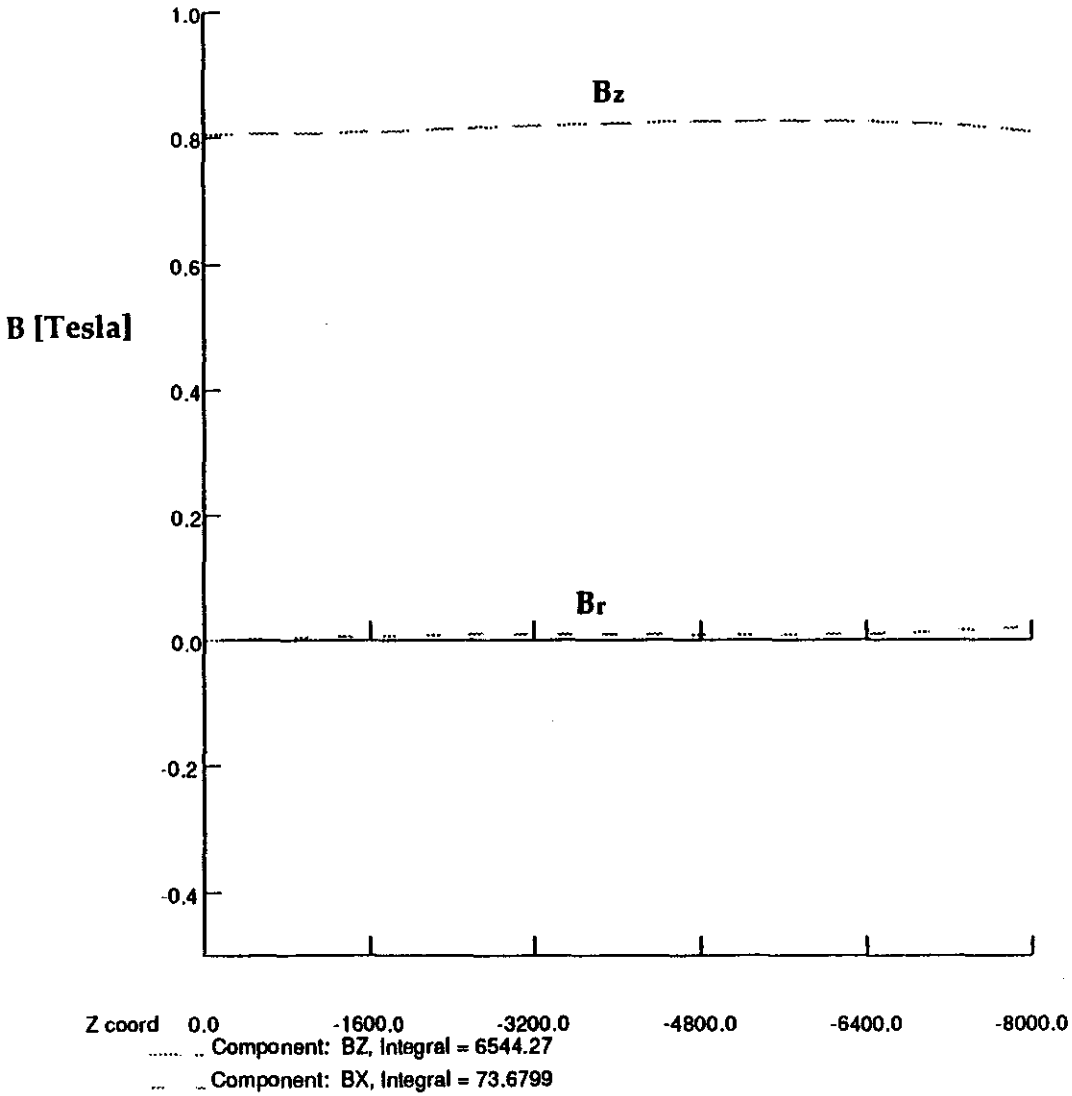

Barrel
R=3854 mm

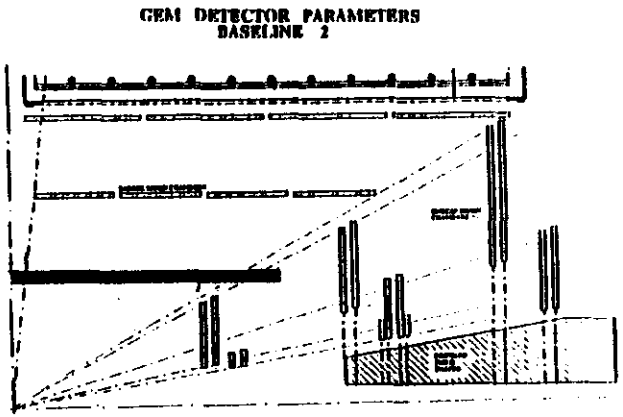

VF/OPERA-3d
(Post-processor)

Fig.6.1

r6282.pic
27/Jul/93 11:51:51 Page 32 : plot comp=bz

Timofeev S.

Barrel
R=6282 mm

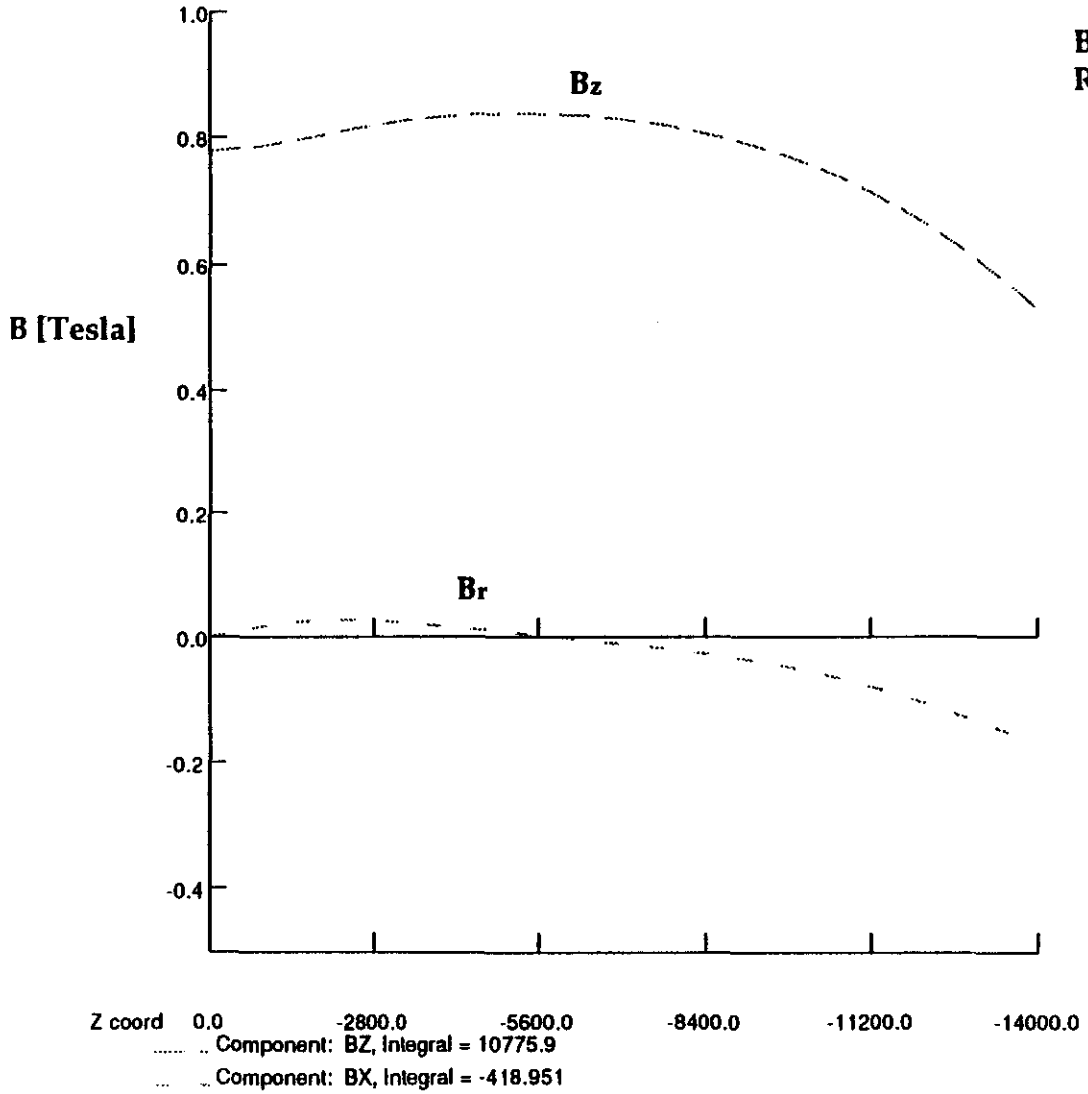

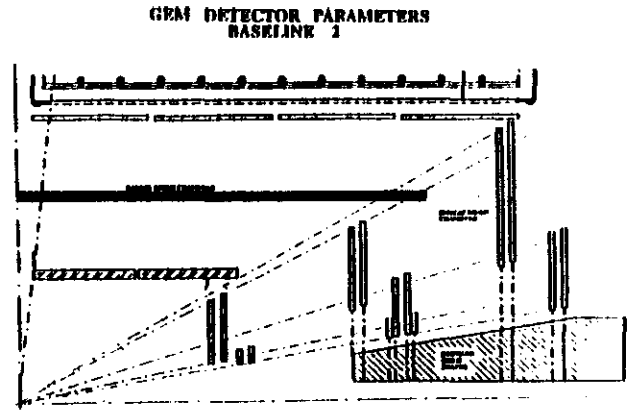

VF/OPERA-3d
(Post-processor)

Fig.6.2

r8588.plc
27/Jul/93 11:46:56 Page 29 : plot comp=bz

Timofeev S.

Barrel
R=8588 mm

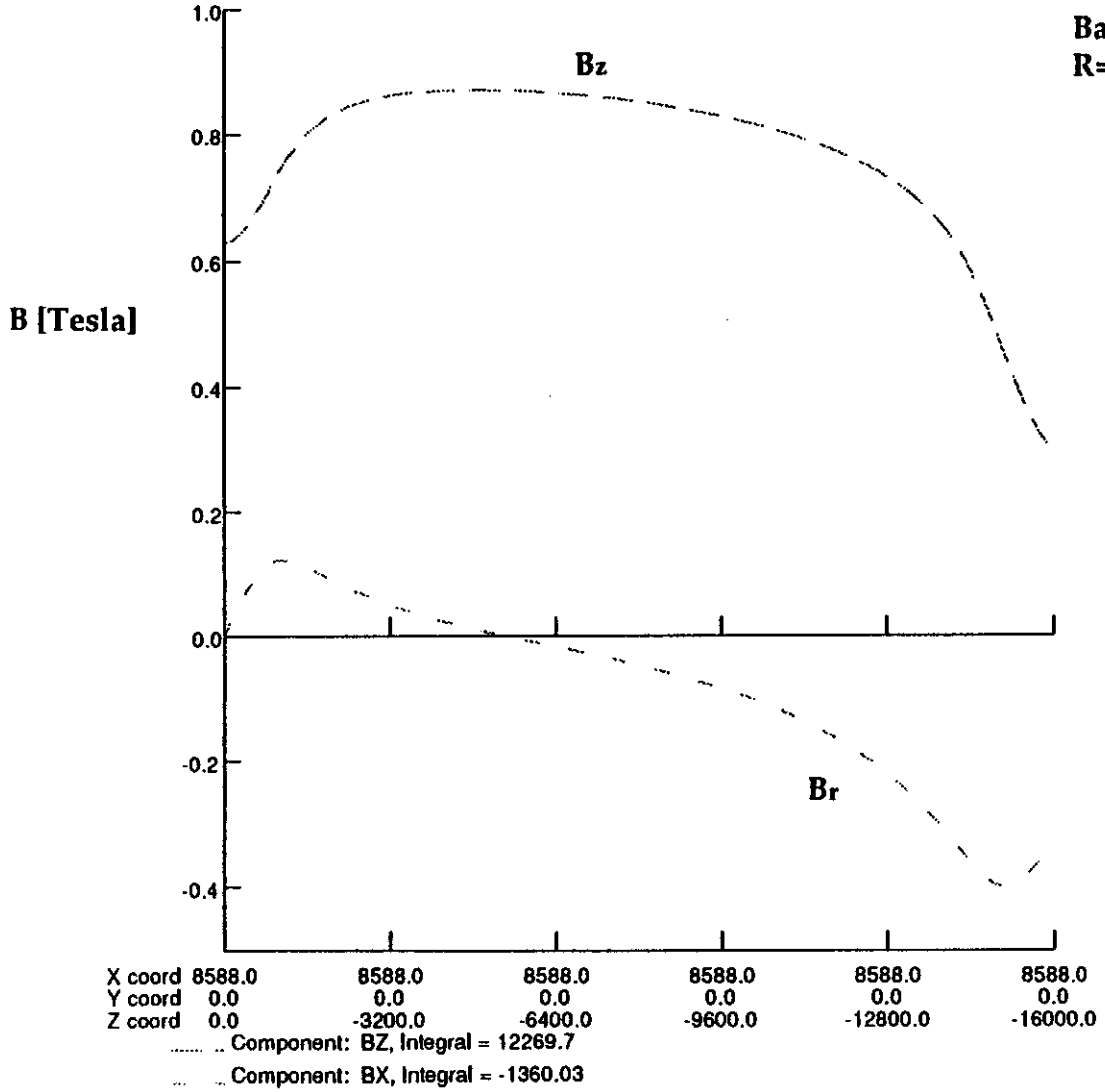

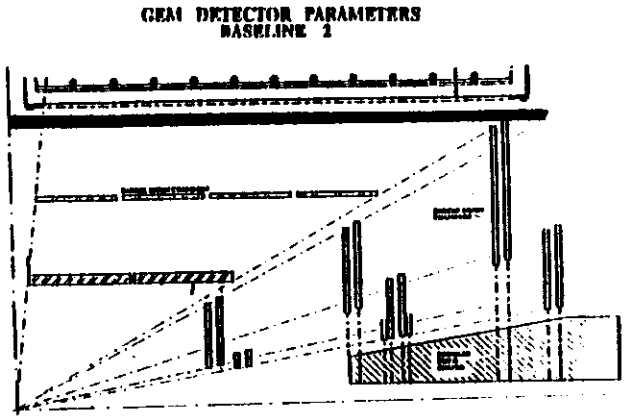

VF/OPERA-3d
(Post-processor)

Fig.6.3

z5760.pic
27/Jul/93 10:23:50 Page 6 : plot

Timofeev S.

Endcap
Z=-5760 mm

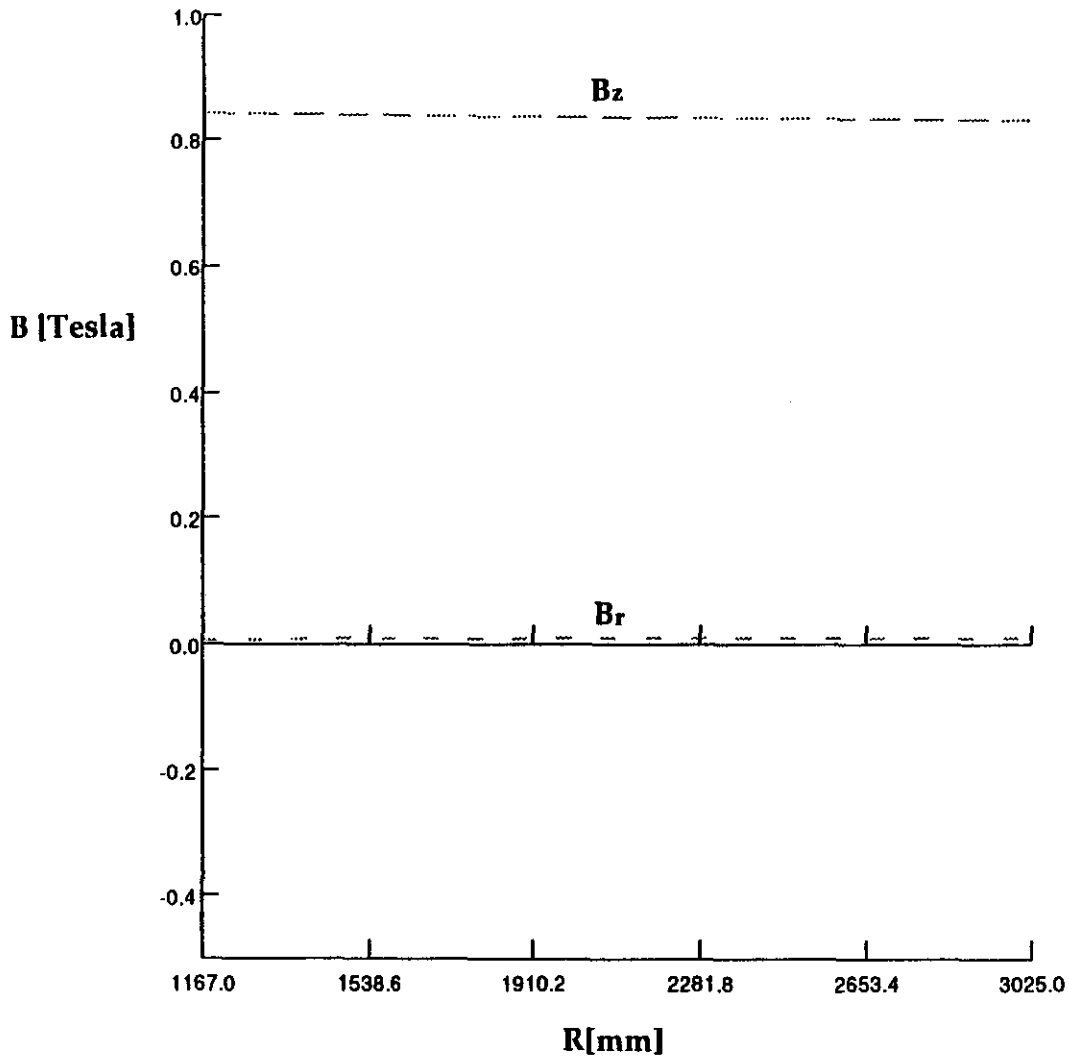

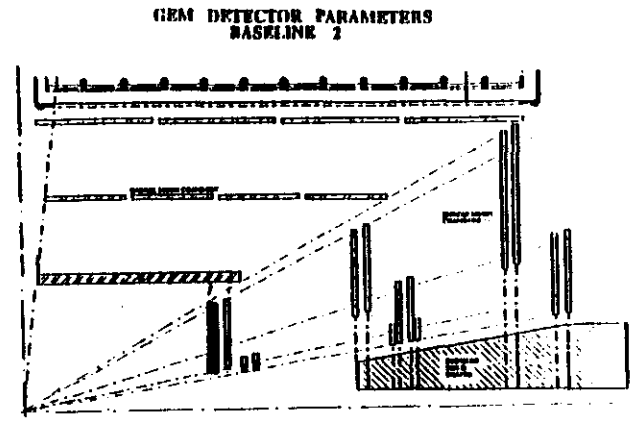

VF/OPERA-3d
(Post-processor)

Fig.7.1

z6600.plc
27/Jul/93 10:26:00 Page 9 : plot comp=bz

Timofeev S.

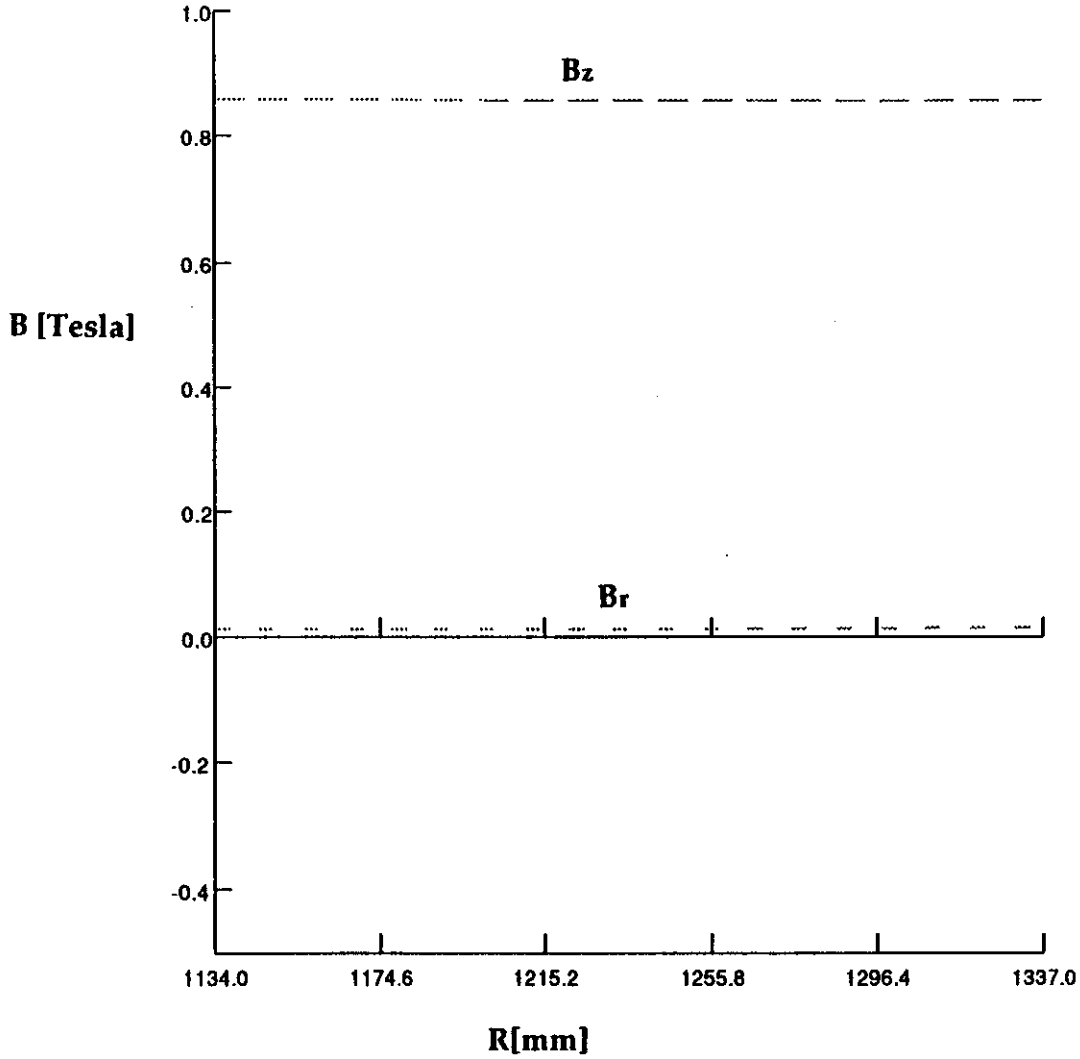

Endcap
Z=-6600 mm

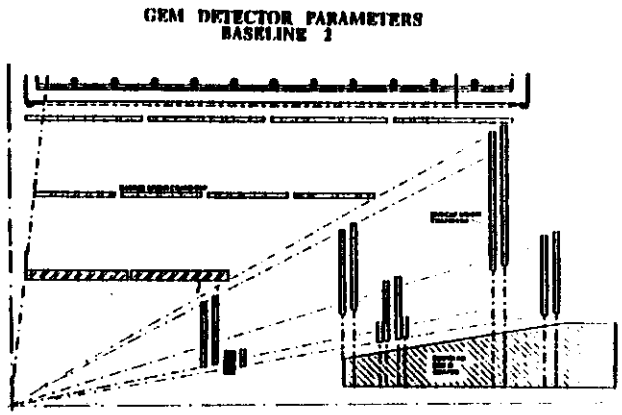

Fig.7.2

VF/OPERA-3d
(Post-processor)

z9950.pic
27/Jul/93 10:28:25 Page 12 : plot comp=bz

Timofeev S.

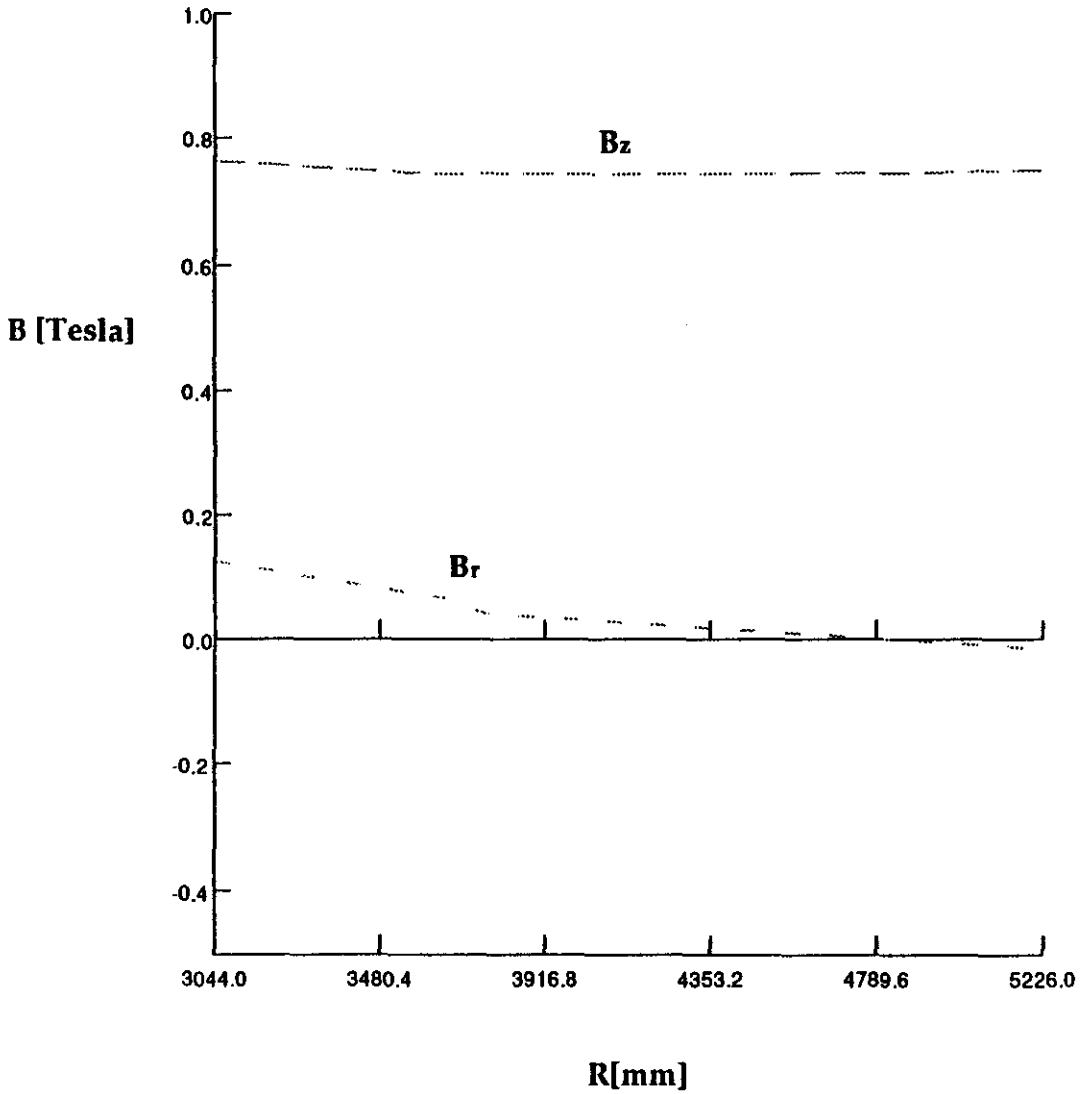

Endcap
Z=-9950 mm

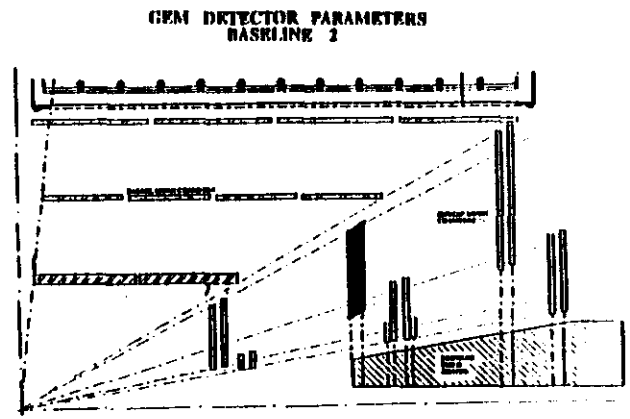

Fig.7.3

VF/OPERA-3d
(Post-processor)

z11250.pic
27/Jul/93 10:30:55 Page 15 : plot comp=bz

Timofeev S.

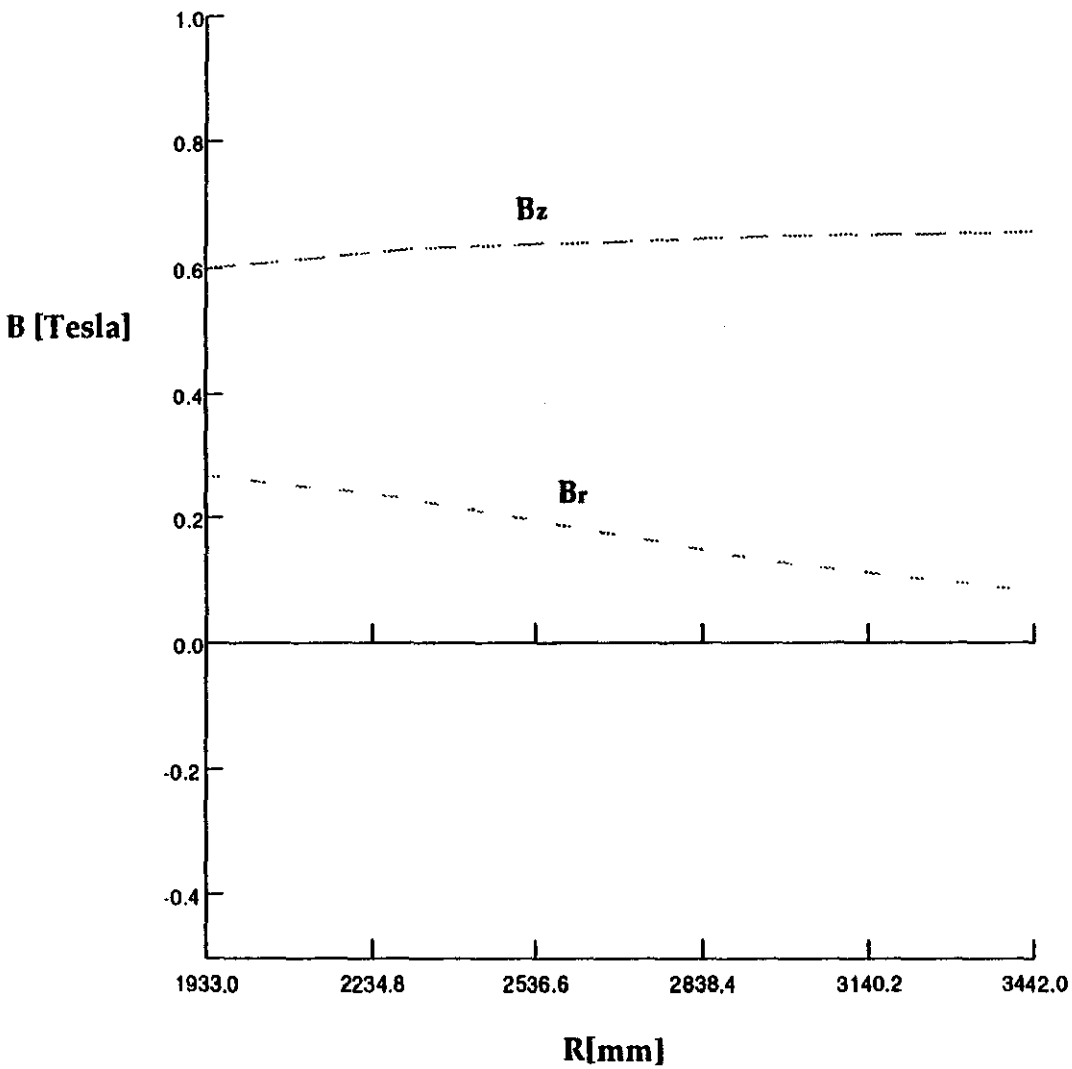

Endcap
Z=-11250 mm

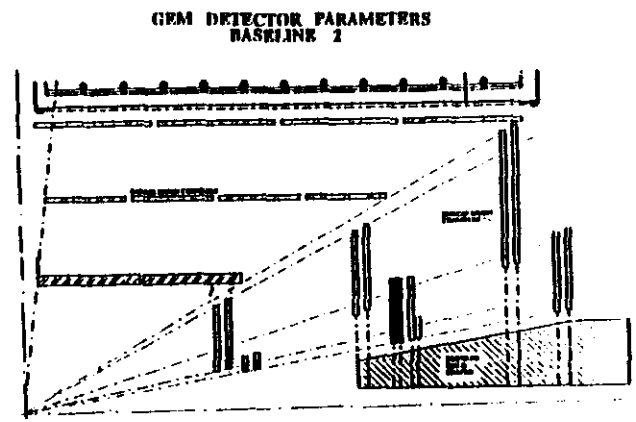

Fig.7.4

VF/OPERA-3d
(Post-processor)

z14750.plc
27/Jul/93 10:40:05 Page 18 : plot comp=bz

Timofeev S.

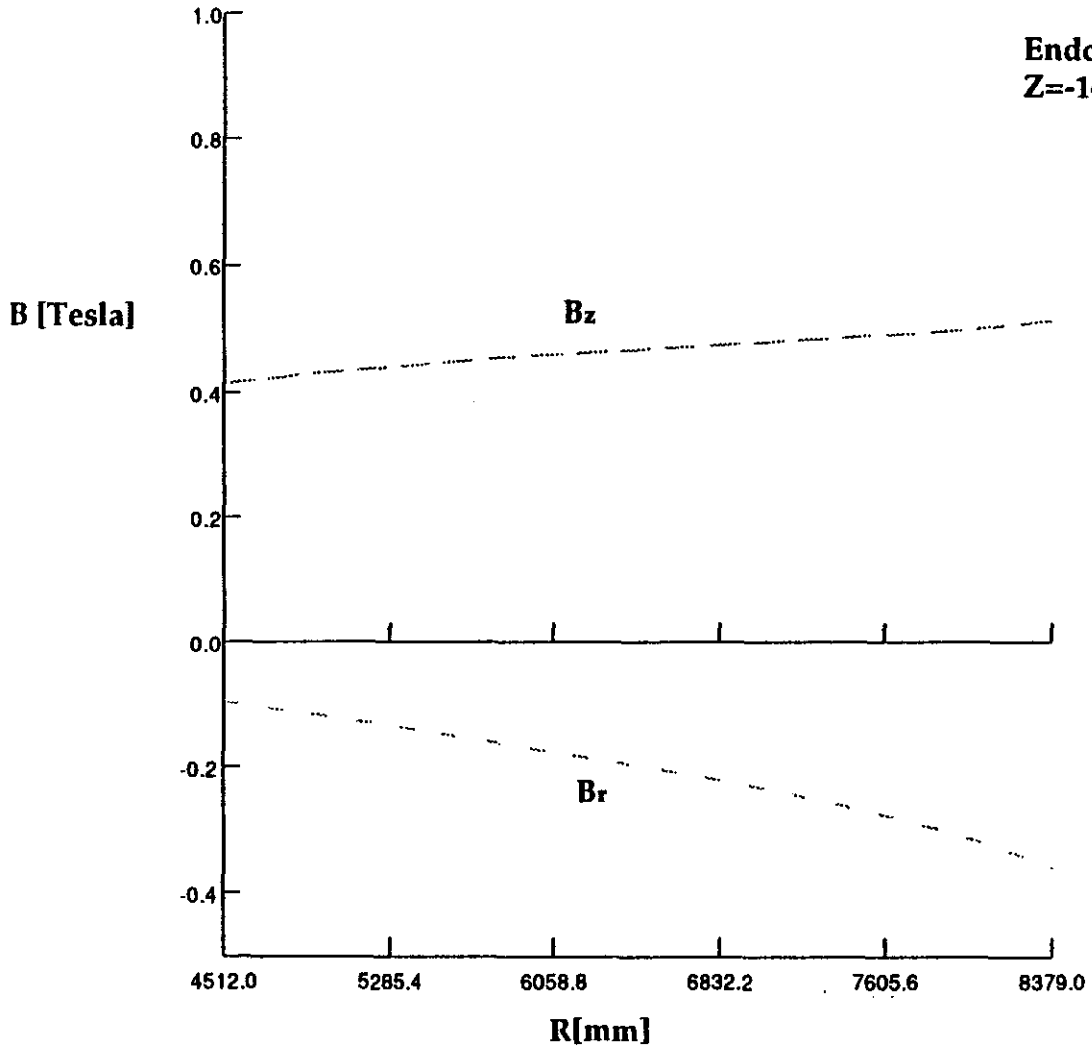

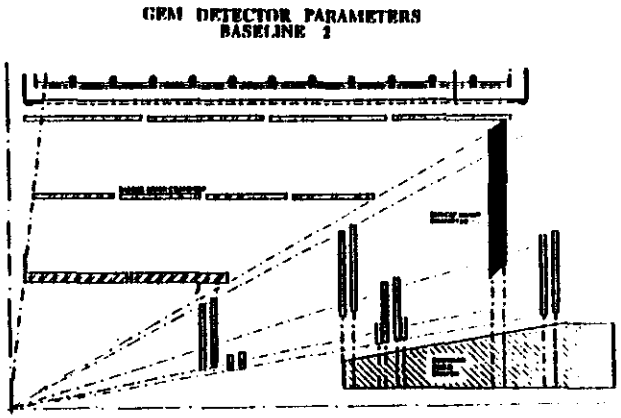

VF/OPERA-3d
(Post-processor)

Fig.7.5

z16250.pic
27/Jul/93 10:42:58 Page 21 : plot comp=bz

Timofeev S.

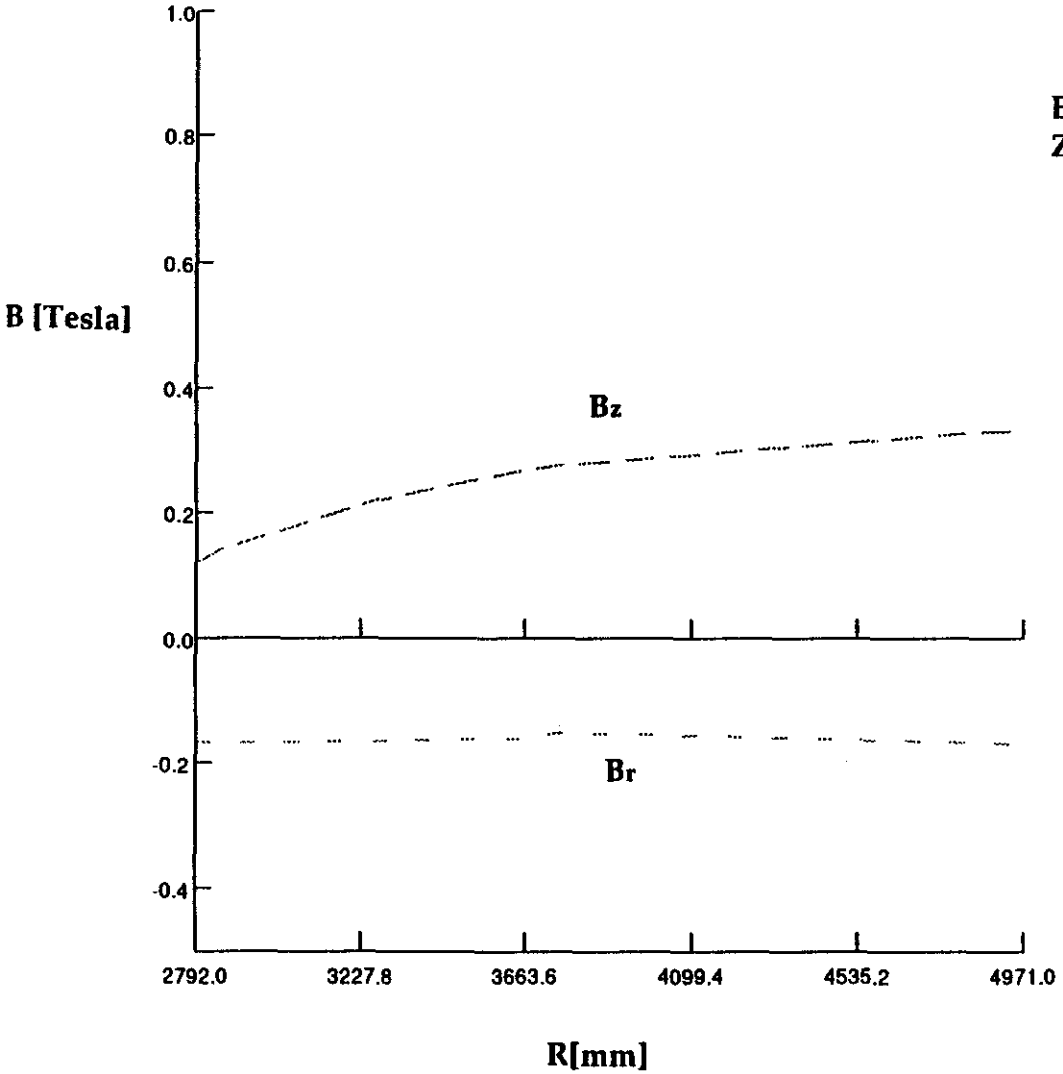

Endcap
Z=-16250 mm

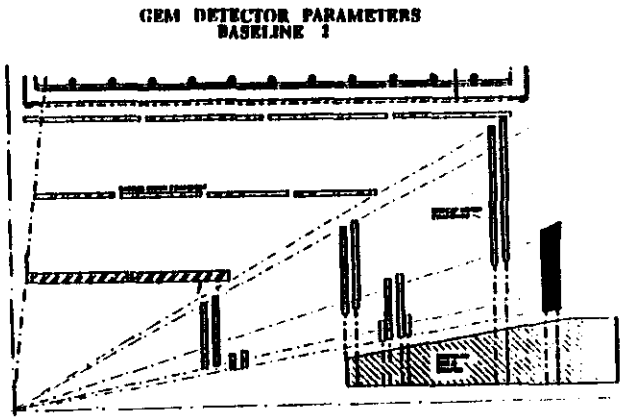

Fig.7.6

VF/OPERA-3d
(Post-processor)

a.pic
29/Jul/93 10:08:18 Page 7 : hist

Timofeev S.

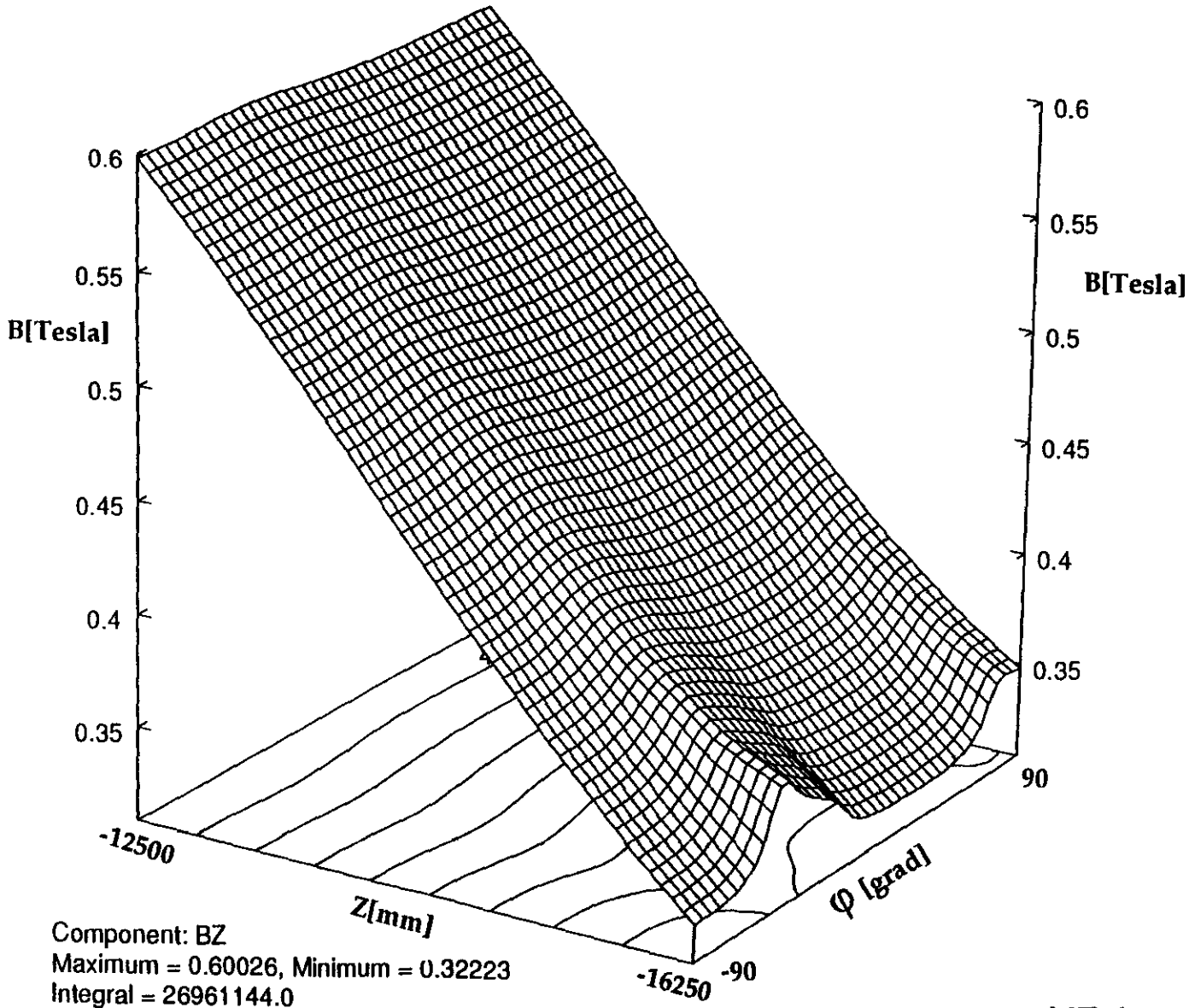

Component: BZ
Maximum = 0.60026, Minimum = 0.32223
Integral = 26961144.0

VF/OPERA-3d
(Post-processor)

Fig.8.1

axial.pic
29/Jul/93 10:13:29 Page 18 : plot

Timofeev S.

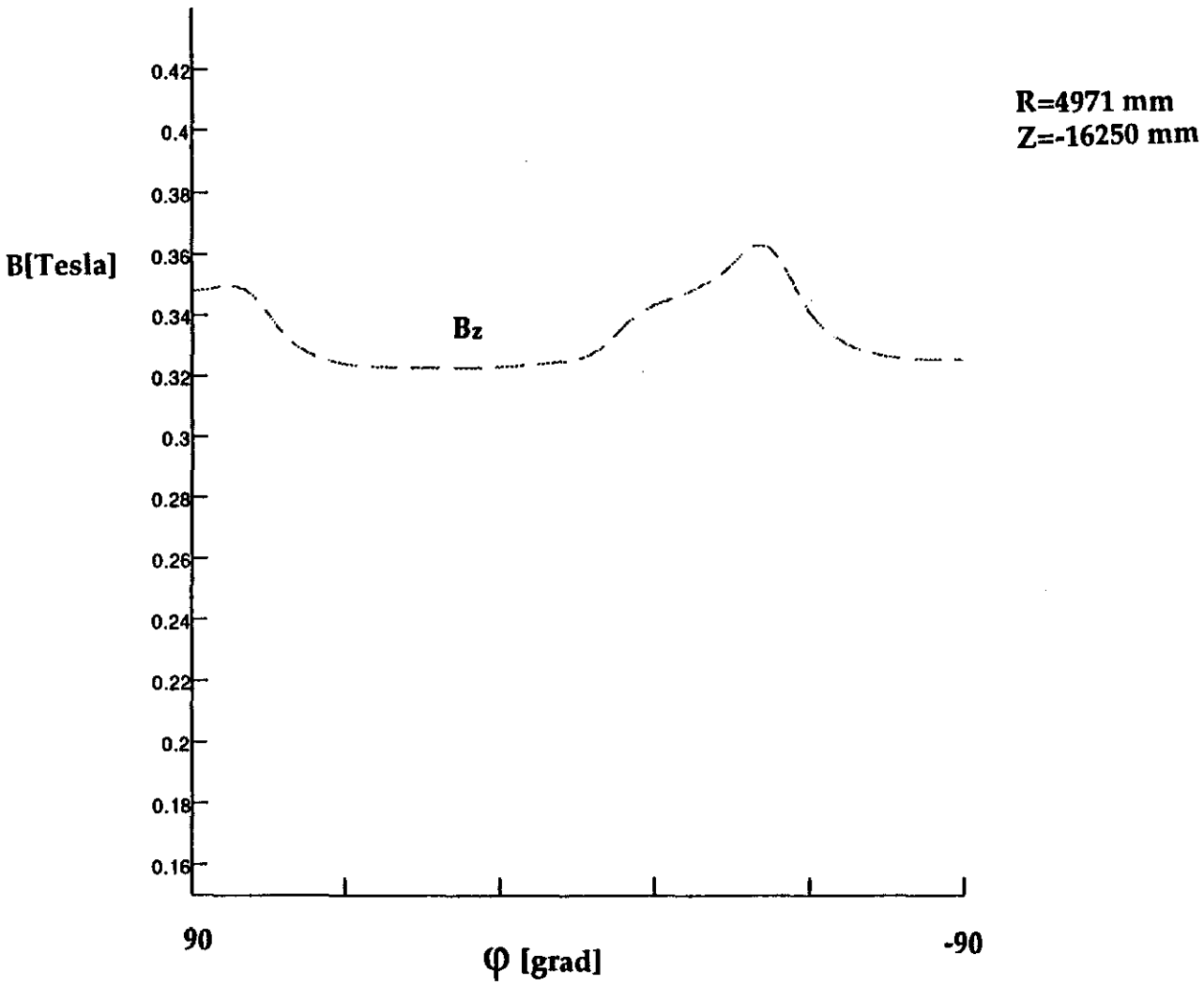

VF/OPERA-3d
(Post-processor)

Fig.8.2

thet90.plc
29/Jul/93 17:46:19 Page 53 : plot comp=bz

θ=90

Timofeev S.

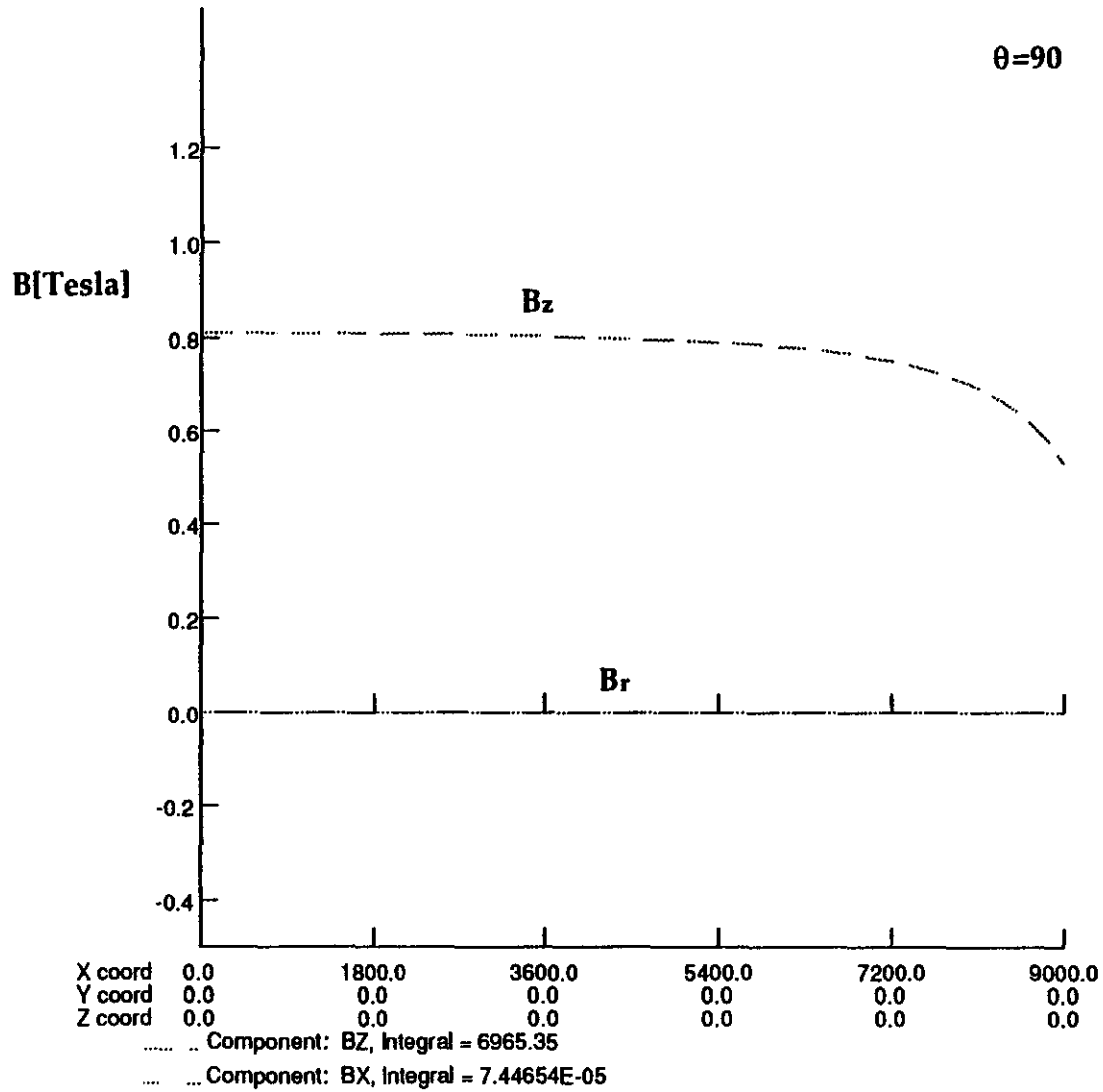

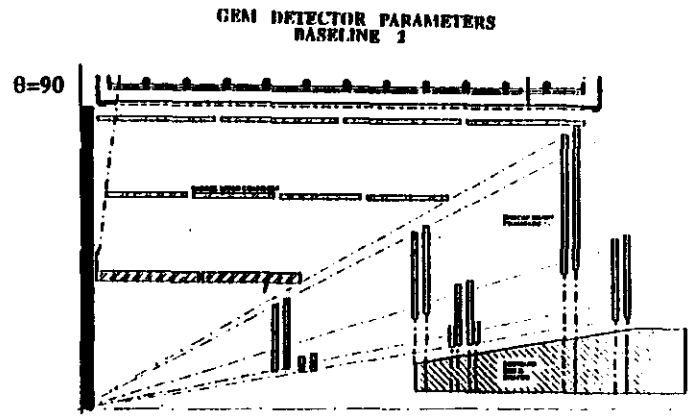

VF/OPERA-3d
(Post-processor)

Fig.9.1

thet29.plc
29/Jul/93 17:51:21 Page 56 : plot

θ=29.60

Timofeev S.

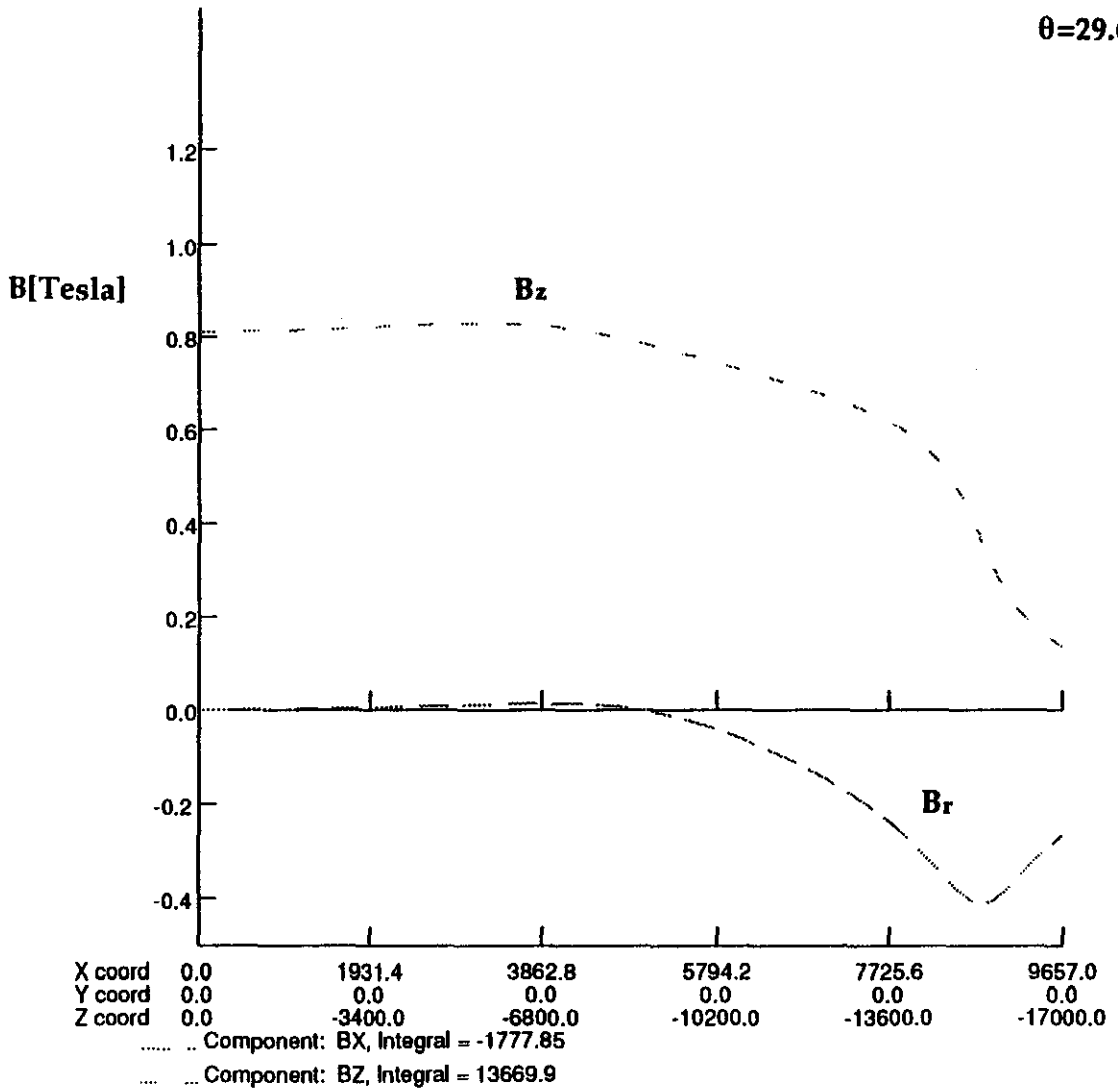

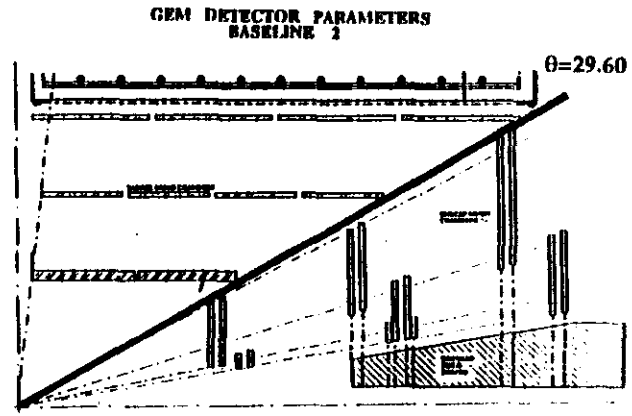

VF/OPERA-3d
(Post-processor)

Fig.9.2

thet17.plc
30/Jul/93 09:15:16 Page 59 : plot

θ=17.01

Timofeev S.

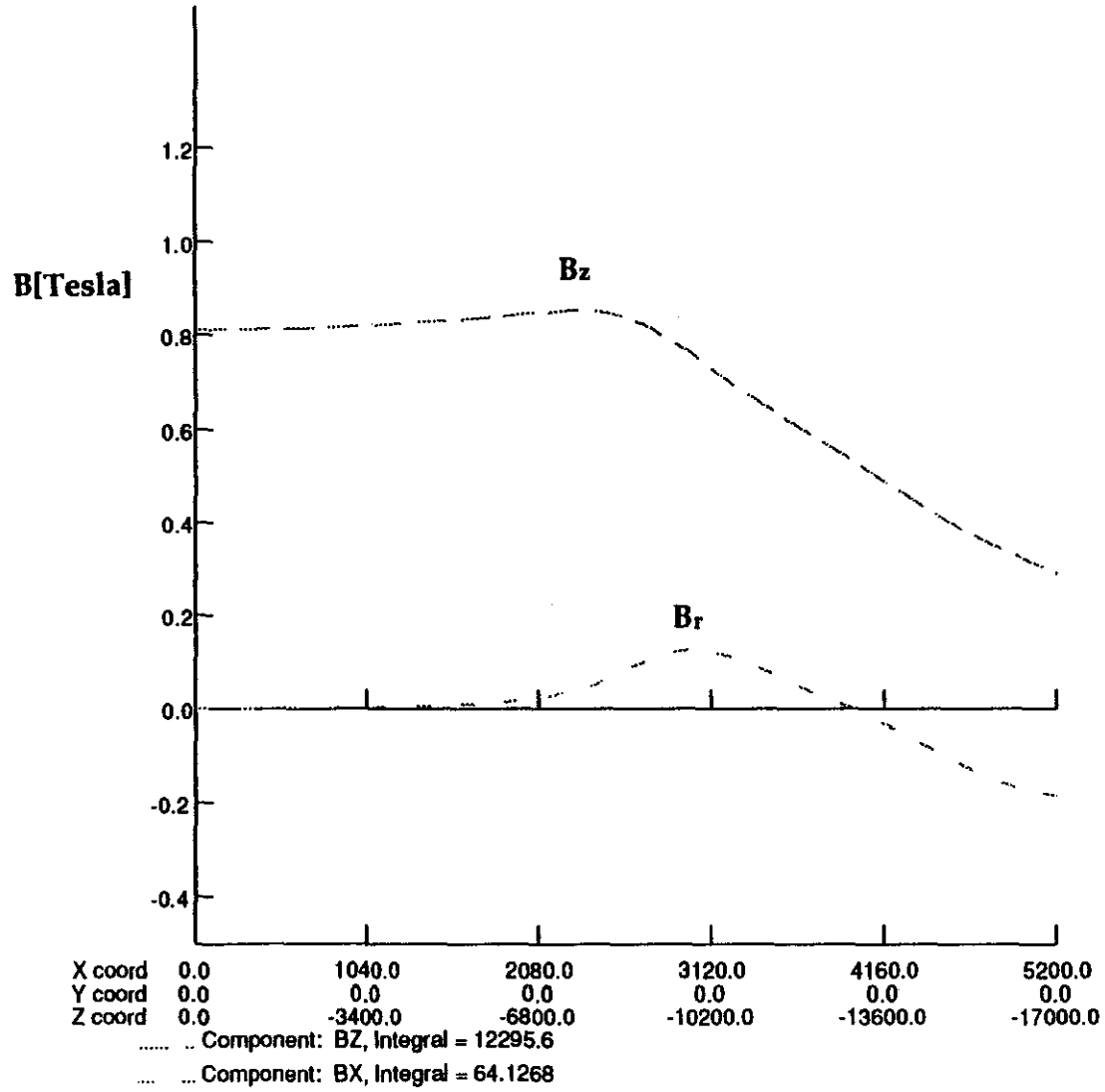

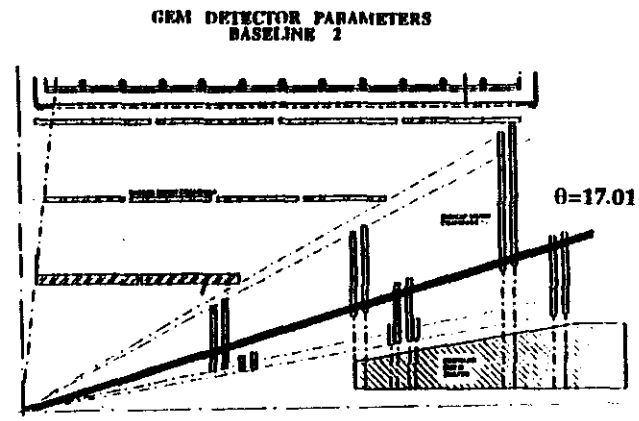

VF/OPERA-3d
(Post-processor)

Fig.9.3

thet9.pic
30/Jul/93 09:19:50 Page 62 : plot comp=bz

θ=9.75

Timofeev S.

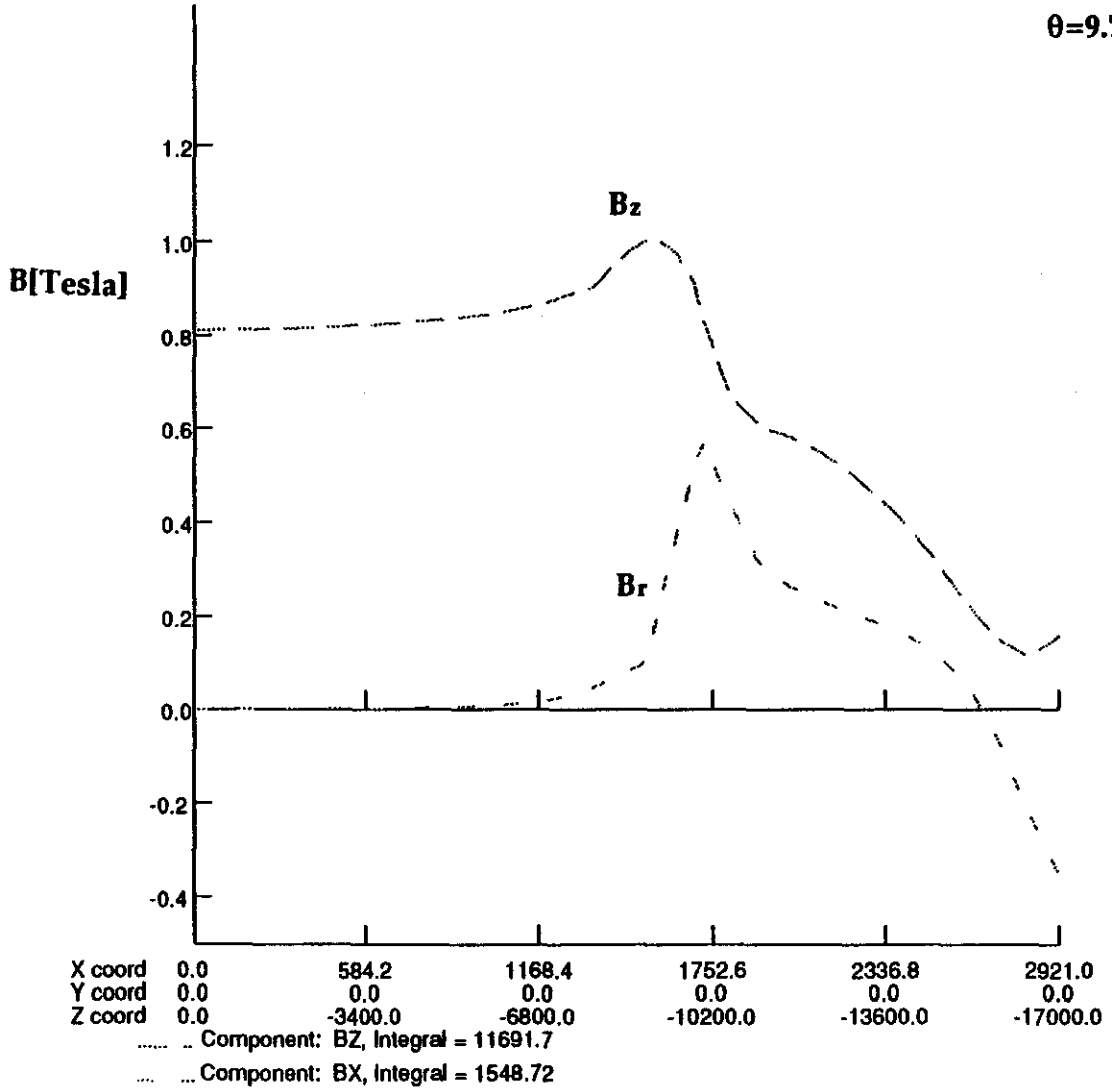

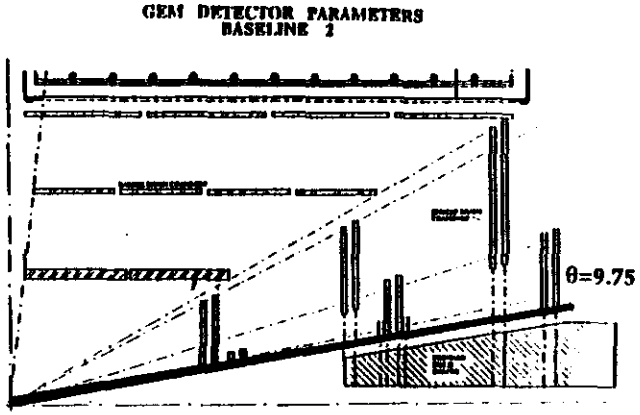

VF/OPERA-3d
(Post-processor)

Fig.9.4

a.plc
30/Jul/93 09:22:24 Page 65 : plot comp=bz

θ=9.45

Timofeev S.

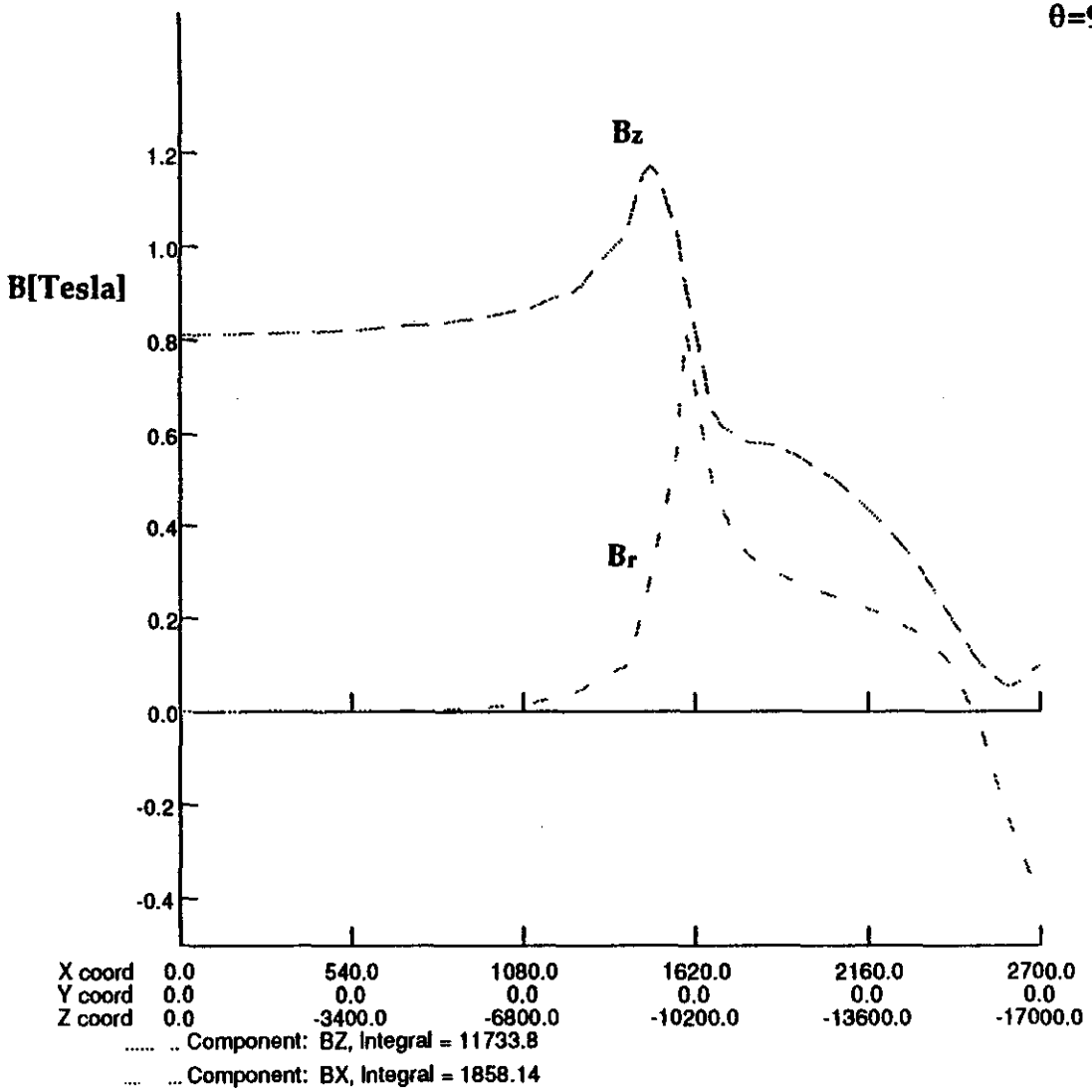

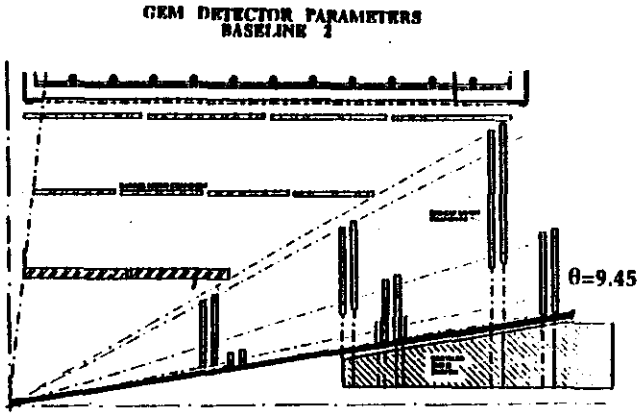

VF/OPERA-3d
(Post-processor)

Fig.9.5

a.pic
30/Jul/93 16:18:40 Page 98 : plot

Timofeev S.

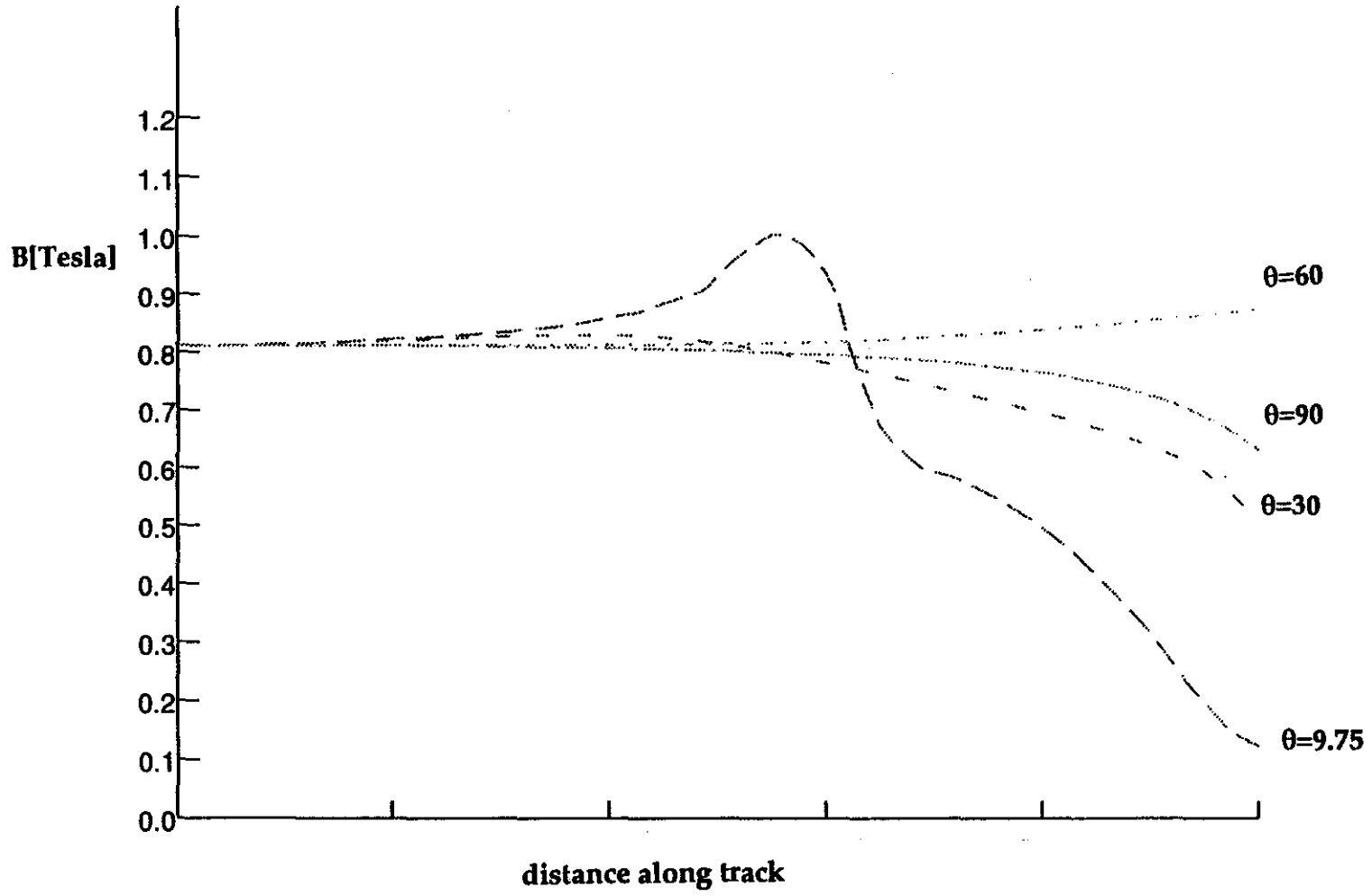

θ=9.75 — — Component: BZ, Integral = 11594.6
θ=30 ... ... Component: BZ, Integral = 13077.6
θ=60 ... . Component: BZ, Integral = 8159.36
θ=90 .... Component: BZ, Integral = 6725.28

VF/OPERA-3d
(Post-processor)

Fig.10